# Preliminary Design Report

Trey Dufrene    Zack Johnson    David Orcutt    Alan Wallingford    Ryan Warner

Submitted in Partial Fulfillment of the Requirements of:

ME407 Preliminary Design – Fall 2019

Meiosis

College of Engineering
Embry-Riddle Aeronautical University
Prescott, AZ

# Contents

# List of Figures



# List of Tables

# List Of Acronyms and Abbreviations

| | |
|---|---|
| FK | Forward Kinematics |
| IK | Inverse Kinematics |
| PD | Proportional Derivative |

# Notation

| | |
|---|---|
| ${}^{\text{Frame}}_{\text{From}}r_{\text{To}}$ | Direction Vectors |
| ${}^{\text{From}}T_{\text{To}}$ | Direction Cosine (Transformation) Matrices |
| $c_{\theta_{nm}}$ | $\cos(\theta_n + \theta_m)$ |
| $s_{\theta_{nm}}$ | $\sin(\theta_n + \theta_m)$ |

# 1 Introduction

# 2 Requirements

The requirements of the system concisely define the capabilities the system must possess in order to solve the stated problem.

## 2.1 Hardware

The following requirements are hardware specific and dictate the physical constraints the system must adhere to.

### 2.1.1 The system shall cost the end-user no more than $1000.

### 2.1.2 The system shall be fully dexterous without being kinematically redundant.

To create a system with the intention of advancing education, it must be complex enough to encourage higher level problem solving, as well as be capable enough (dexterous) in a broad spectrum of tasks — in the interest of remaining useful in addition to retaining the interest of students.

### 2.1.3 The system end effector shall maintain a positional accuracy magnitude of $\pm 1$ mm and an orientation accuracy of $\pm 5°$ eigen angle from the base frame.

To ensure that the robot has educational value, the accuracy must be defined so that any desired positions and movements are achieved.

### 2.1.4 The system end effector shall maintain a pose repeatability magnitude between 0.1—1.5 mm for the position and $\pm 4°$ eigen angle from the base frame for the orientation.

This is to ensure a robot that can execute the same movement commands repeatedly and have the same results every time.

### 2.1.5 The system's reachable workspace shall be a hemisphere with a radius of 300-700 mm.

This workspace will provide enough movement to manipulate objects in order to perform basic tasks.

#### 2.1.6 The system's dexterous workspace shall contain a hemispherical shell within the reachable workspace with a thickness of 280 mm.

#### 2.1.7 The system shall have a removable end effector capable of picking and placing a low-odor chisel tip Expo dry erase marker.

This creates a robot capable of performing a variety of basic tasks, which enhances its educational value.

#### 2.1.8 The system shall be able to write with a low-odor chisel tip Expo dry erase marker.

### 2.2 Software

#### 2.2.1 The system shall be open source.

This will create an easily obtainable, low cost method of distributing the system's source code, which may be modified for personal use.

#### 2.2.2 The system shall be capable of operating given only desired end effector cartesian coordinates specified with respect to the base frame.

This simplicity makes the system of use to inexperienced users.

# 3 Conceptual Design

The terminator T-2000 is a science-fiction spectacle of a robot – until you see the price. Channeling the inspiration many high school students may have for robotics, MEIOSIS robotics aims to provide an affordable manipulator to educators and enthusiasts. MEIOSIS uses primarily 3-D printed components and easily accessible materials. Among these materials are a Raspberry PI, smart servos and metal tubing. These features create an open-source manipulator accessible to the public to further robotics education.

## 3.1 Physical System Overview

The physical design of the robotic manipulator will be shown through Figures *1, 2, 3,* and *4*.

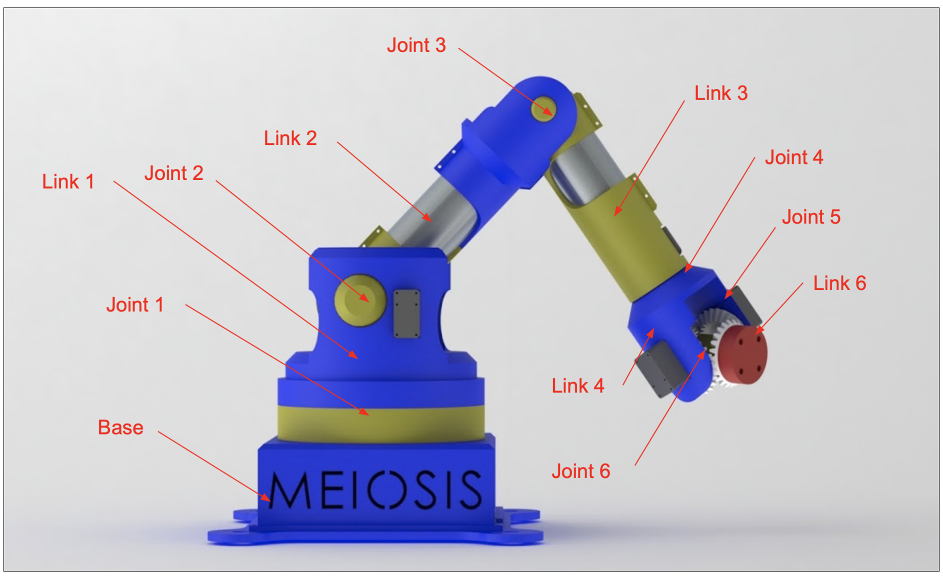


Figure 1: Overall System Conceptual Design

The colored links in *Figure 1* distinguish the different joints and links of the manipulator. The overall reach of the robot will be 582.5 mm. This length was chosen to decrease material cost and weight while still satisfying requirement 2.1.2 and 2.1.5, allowing the manipulating to pick and place objects to perform basic tasks. The base of the robot will be made to contain the Raspberry Pi and other electrical components.

### 3.1.1 Base

The base of the manipulator will house several of the electronic components, such as the computational system, power supply, and motor controller. A cross section of the base can be seen in *Figure 2*.

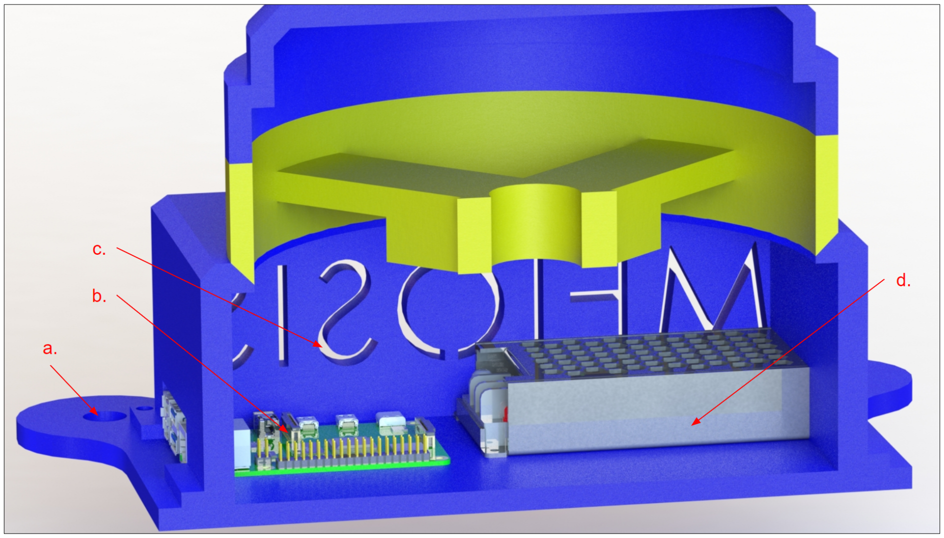


Figure 2: Manipulator Base with Call-outs

From *Figure 2*,

*a. Base Supports:* The base supports are located at each corner of the base and will allow the base of the manipulator to be securely attached to a variety of surfaces with either standard bolt/fastener hardware or suction cups.

*b. Computational System:* The computational system will be a Raspberry Pi; it will be housed in the base, which allows the Raspberry Pi to be more easily accessible. The primary reason for this system being chosen is to fulfill the budget requirement, 2.1.1. The Raspberry Pi will compute the manipulator's kinematics and command the motors accordingly.

*c. Airflow Cutouts:* The side of the base will have cutouts to allow for airflow through the base; since the power supply is housed inside of the base as well as the computational system, the temperature must be regulated to prevent overheating.

*d. Power Supply:* The power supply will be housed in the base as well; this allows the power supply to be more accessible and therefore more modifiable, so the end-user can easily expand the system to fulfill their needs.

### 3.1.2 Links

*Figure 3* is an image of the robot that shows the links and their key features.

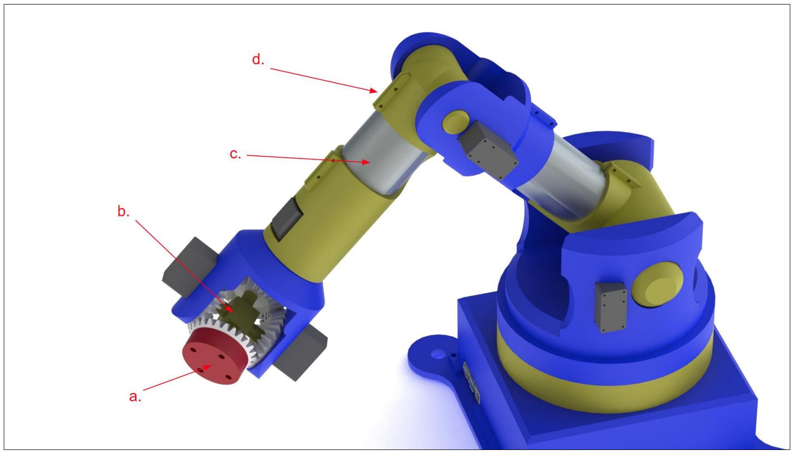


Figure 3: Drawing Showing Key Features of Design

*Figure 3* highlights a few of the key features of our design. Call-out a shows the connection point for the end effector. The mountings are the standard used by the Sawyer manipulator. This may be adjusted to accommodate lower cost, more accessible end effectors. Call-out (b) shows the differential gearbox that will be used in the manipulator's wrist, saving space and weight. The manipulator will have aluminum tubing as support in the links (c) and will be attached to the 3D printed portion of the robot using clamp joints (d) tightened by screws.

*Figure 4* is an image of the cross section of link 2 for the manipulator.

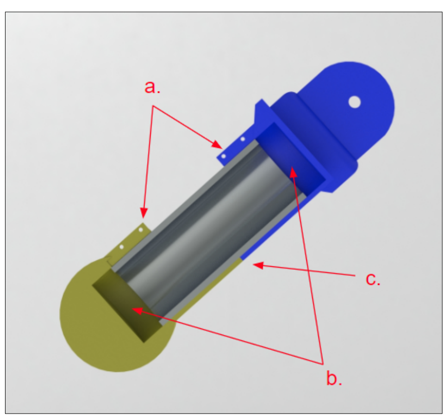


Figure 4: Drawing Showing Link Cross Section

The cross section seen in *Figure 4* shows the internal design for links two and three. It features two clamps that hold a hollow aluminum bar in place (a) and allows for gaps between the aluminum tube and the 3D printed call-out (b). The proper length will be dictated by the 3D printed guides lining up at call-out (c). This allows for imprecision in the manufacturing of the aluminum tube.

## 3.2 System Functions

The system can be divided into two subsystems: the electrical and software systems. The electrical subsystem includes the wiring and hardware computational components, power system, actuators with drivers, and sensors. The software subsystem includes the algorithm for the computational system.

## 3.3 Electrical

*Figure 5* is the block diagram for the electrical system of the manipulator.

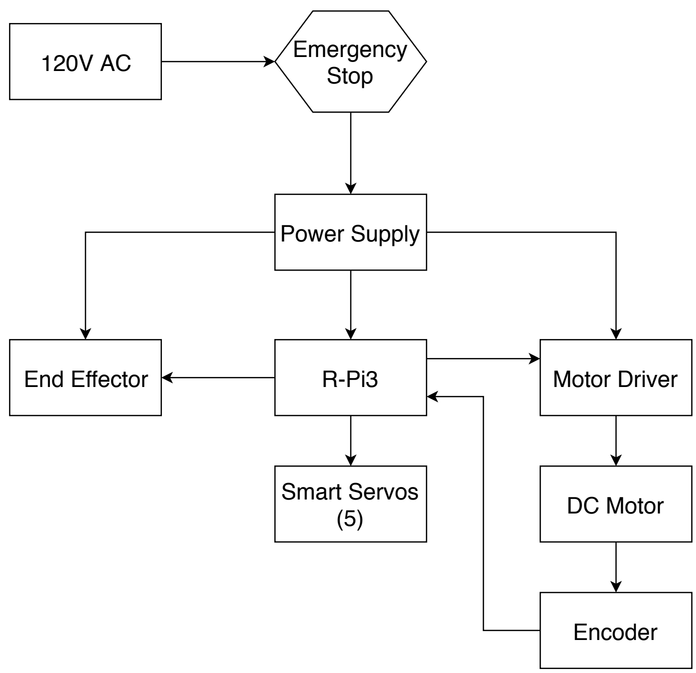


Figure 5: Electrical System Block Diagram

*Figure 5* shows that the electrical systems of the manipulator will be relatively simple. Power is supplied by the 120V AC from standard wall outlets. A power supply will adapt the AC voltage to the required voltages for each component. One component is the Raspberry Pi, which will perform calculations for motor control (described below in software). It will send signals to the DC motor driver and the five smart servos. The smart servos have an on-board controller, so no feedback will be necessary. However, the first joint, between the base and the first link, will be actuated by a DC motor with an encoder to minimize cost.

## 3.4 Software

*Figure 6* shows the software flowchart for the system.

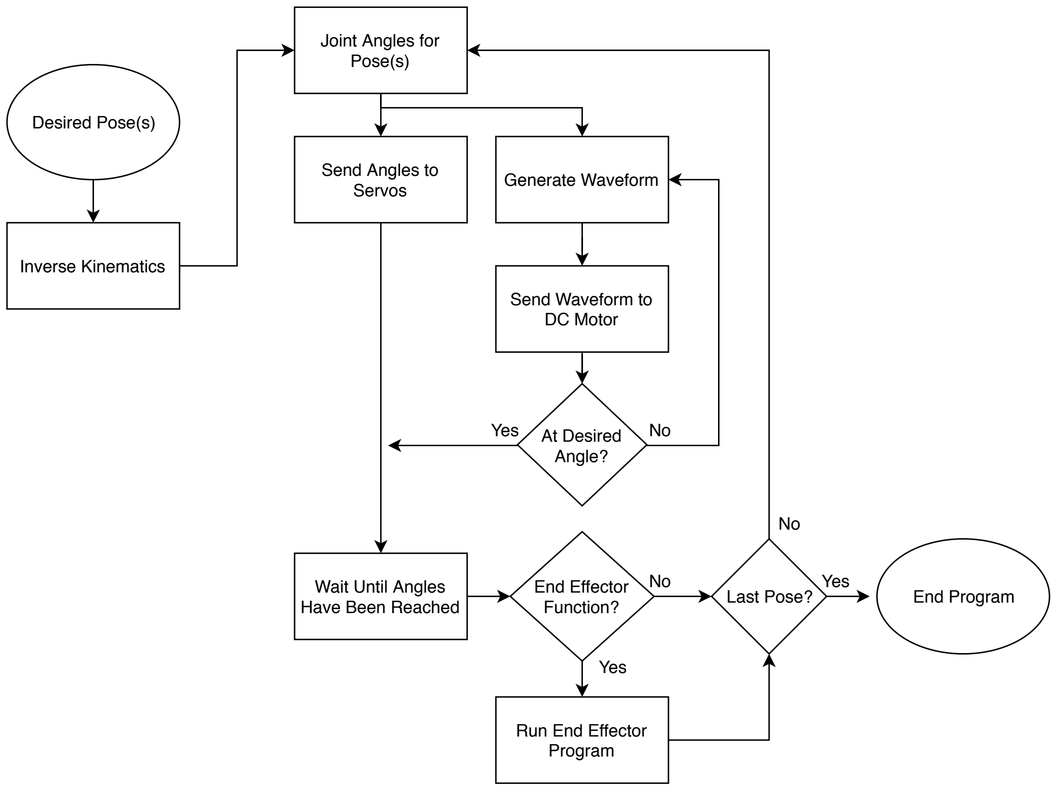


Figure 6: Software Flowchart

Similar to the electrical system, the software is also simple. *Figure 6* shows that the software will receive the desired pose or poses the user would like the manipulator to reach. Then the Raspberry Pi will use inverse kinematics to calculate the necessary joint angles. The waveforms/desired angles will be sent to the respective drivers/motors, and positional information will be sent back to the Raspberry Pi to adjust the DC motor angle. When the motors have reached their desired pose, the Raspberry Pi will actuate the end effector if it is specified by the user. The system will then check to see if there are any more poses to reach and either repeat the motor control section given the desired angles of the new pose or end program if the last pose has been reached.

# 4 Specifications

With the intention of making robotics education more accessible, The Manipulator for Educational Institutions with Open Source Integrated Systems (MEIOSIS) intends to provide high school educators and robot enthusiasts with a low cost manipulator. The system should be usable by novice students. It should also be modifiable to create a sustainably increased understanding of robotics. While MEIOSIS may not fully emulate industrial manipulators, it aims to provide more students with access to robotics education.

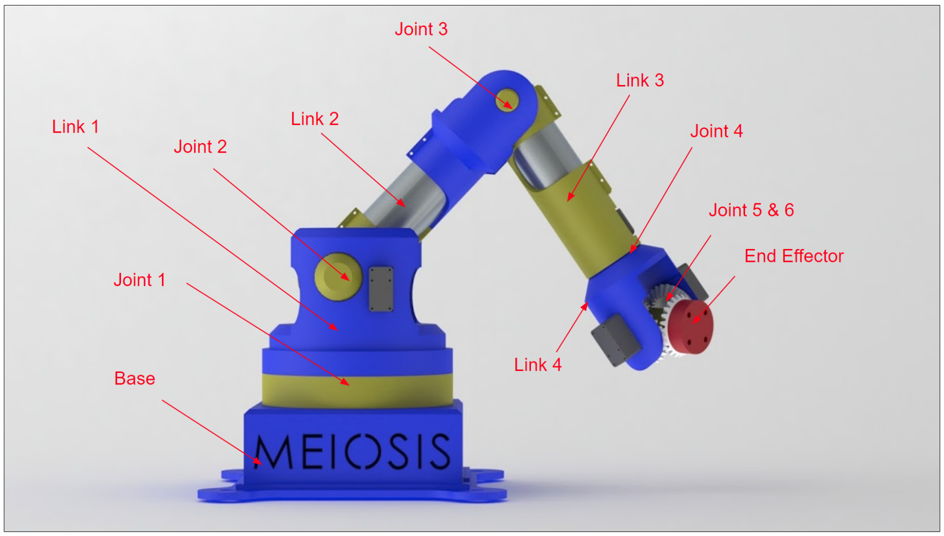


Figure 7: Overview of Physical System

The design seen in *Figure 7* is based on our conceptual design. It features four links and six joints for rotation and will be referenced throughout this document. The base of the manipulator and end-effector can also be seen in the figure.

## 4.1 Design Requirements

The specifications of the system are strictly based on the requirements defined previously. The requirements are divided into two primary categories, hardware and software.

## 4.2 Hardware

The following requirements and specifications are hardware specific and dictate the physical constaints the system must adhere to.

### 4.2.1 The system shall cost the end-user no more than $1000.

*4.2.1.a The cost for the MEIOSIS team to develop the manipulator shall cost no more than $800.*

### 4.2.2 The system shall be fully dexterous without being kinematically redundant.

*4.2.2.a The system shall consist of six rotational joints connected by four links. The last three joints will create a spherical wrist.*

As defined [1], “A manipulator having more than six DOF is referred to as a kinematically redundant manipulator (5).” A manipulator with less than six degrees of freedom will not be fully dexterous within it’s workspace. *Figure 9* (see subsection 4.2.6, p. 11) shows a six degree-of-freedom rotary manipulator with it’s coordinate frames in zeroed positions. The joint and link locations are seen in *Figure 7* (see section 4, p. 8).

*4.2.2.b The system shall have no link offsets.*

Link offsets as seen in *Figure 8* are commonly used to avoid singularities. However, having a link offset prevents the manipulator’s dexterous workspace from being a complete hemispherical shell.


Figure 8: Elbow Manipulator Configuration with Link Offset [1]

As shown in *Figure 8*, the line directly above the first joint of the manipulator is offset such that the axes of the other joints are unable to become collinear with the base axis; this prevents singularity but causes a void in the detxterous workspace.

### 4.2.3 The system end effector shall maintain a positional accuracy magnitude of $\pm 1$ mm and an orientation accuracy of $\pm 5°$ eigen angle from the base frame.

To ensure that the robot has educational value, the accuracy must be defined so that any desired positions and movements are achieved.

*4.2.3.a The system shall accommodate a process in which the end user can calibrate the end effector position and orientation to within 0.5 mm and 1 degree of the manipulator's precision.*

The addition of a calibration process allows the removal of any systematic errors, such as drift. The theoretical limit of the calibration process is the difference between the precision and accuracy metrics of the system.

### 4.2.4 The system end effector shall maintain a pose repeatability magnitude between 0.1—1.5 mm for the position and $\pm 4^\circ$ eigen angle from the base frame for the orientation.

*4.2.4.a Joint one and two of the system shall possess an angle error of no more than .025 degrees.*

Being that joint one and two are the first two rotational elements in the system, their error will propagate the most to the end effector's position.

*4.2.4.b Joint three of the system shall possess an angle error of no more than .03 degrees.*

Since joint three is closer to the end effector it's error will not propagate as severely throughout the system.

*4.2.4.c Joints four, five, and six shall possess an angle error of no more than .29 degrees.*

The spherical wrist is the closest to the end effector's final position and therefore has the least error propagation.

### 4.2.5 The system's reachable workspace shall be a hemisphere with a radius of 300-700 mm.

This workspace will provide enough movement to manipulate objects in order to perform basic tasks.

*4.2.5.a The length of link one, two, three, four, and the wrist shall be 220.8 mm, 250 mm, 200 mm, 80 mm, and 52.5 mm respectively.*

This results in a total height of 220.8 mm with a total reach of 582.5 mm in the zeroed configuration as shown in the configuration represented in *Figure 9*.

### 4.2.6 The system's dexterous workspace shall contain a hemispherical shell within the reachable workspace with a thickness of 280 mm.

This workspace will provide enough movement to manipulate objects in order to perform basic tasks. 280mm is slightly greater than the length of letter paper.

*4.2.6.a The rotational limit of joint one, two, three, four, five, and six shall be* $\pm 180°$, $-9.7°$ *to* $177.5°$, $-150.6°$ *to* $-19.3°$, $\pm 180°$, $-180°$ *to* $-1.6°$, *and* $\pm 180°$ *respectively.*

The angles stated are with respect to the kinematic model shown in *Figure 9.* To be fully dexterous within our 280 mm dexterous workspace the manipulator must have the joint angles specified above. The joint limitations were calculated by iteratively verifying the orientation about every point within the quarter hemisphere cross section seen in *Figure 22* (see Appendix, p. 34).

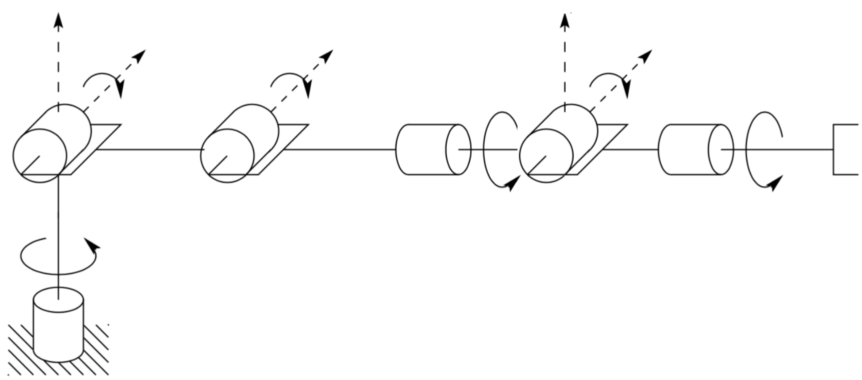

Figure 9: Kinematic Model Representing Zeroed Configuration [1]

### 4.2.7 The system shall have a removable end effector capable of picking and placing a low-odor chisel tip Expo dry erase marker.

This creates a robot capable of performing a variety of basic tasks, which enhances its educational value.

*4.2.7.a The system shall use a parallel gripper that can close to 18mm.*

The diameter of a low-odor chisel tip Expo dry erase marker is approximately 18 mm.

*4.2.7.b The end effector shall attach to the manipulator using screws configured in a pattern that can accommodate a Dynamixel AX-12A servo.*

It is expected that a majority of end effector styles will have to accommodate for a servo to facilitate actuation, therefore a pattern was chosen to standardize the mounting.

### 4.2.8 The system shall be able to write with a low-odor chisel tip Expo dry erase marker.

*4.2.8.a The end effector shall be able to support 0.004 Newton meter moments about the axes normal to its gripping surfaces.*

The coefficient of friction between the Expo marker and paper can be approximated and given the weight of an Expo marker the approximate grip strength of the end effector can be calculated.

## 4.3 Software

The following requirements and specifications are software specific and determine the attributes of the operating system.

### 4.3.1 The system shall be open source.

This will create an easily obtainable, low cost method of distributing the system's source code, which may be modified for personal use.

*4.3.1.a The software shall be hosted publicly on an online repository and maintain an MIT license for distribution.*

This allows the end-user to freely download and modify the code without licensing. The MIT license disregards any legal obligation to code upkeep and documentation by the original author.

### 4.3.2 The system shall be capable of operating given only desired end effector cartesian coordinates specified with respect to the base frame.

*4.3.2.a The system shall have a user interface capable of accepting the end-effector's desired cartesian position and Euler angle orientation as a six element row vector.*

The system software interface facilitates an untrained user to operate without the advanced knoledge of the system's kinematics.

*4.3.2.b The system shall be capable of performing floating point arithmetic.*

The solution for the inverse kinematics requires the ability to perform high level arithmetic with little error.

# 5 Preliminary Design

## 5.1 CAD

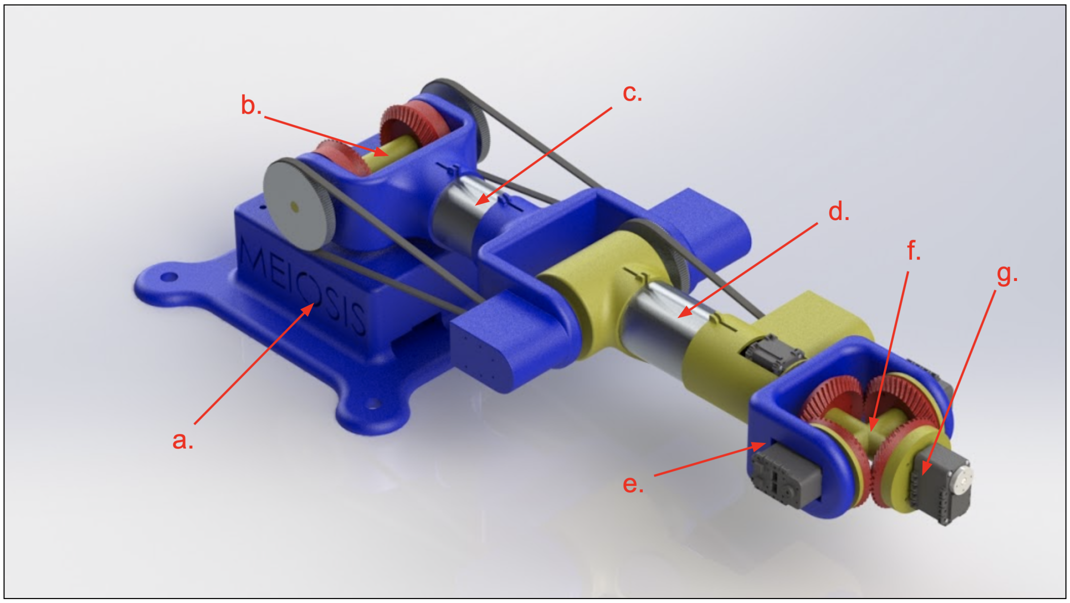


Figure 10: Overall Model Render with Callouts

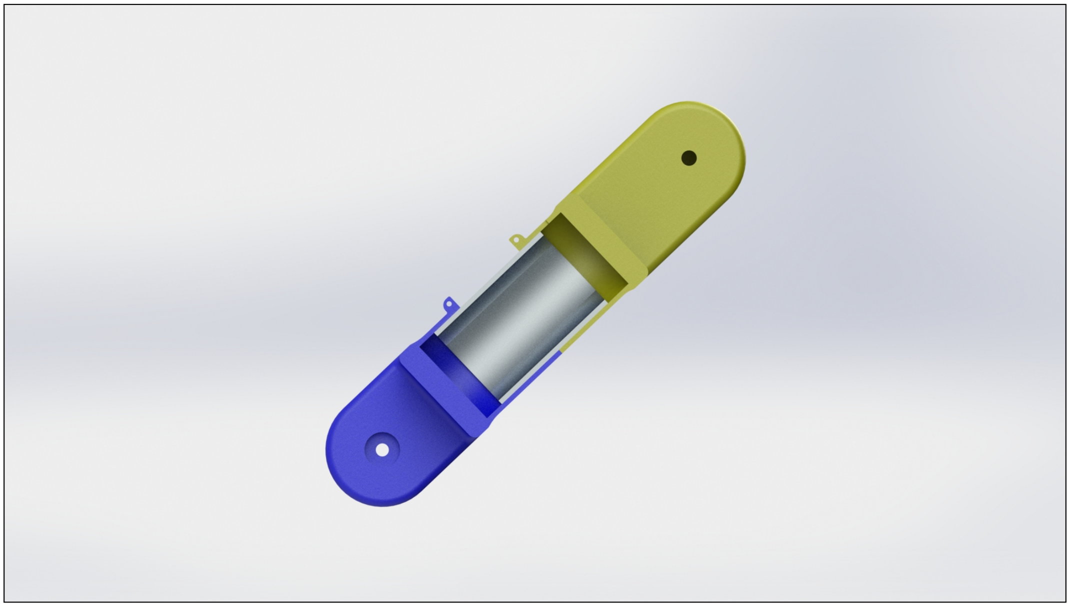

Figure 11: Link Cross Section

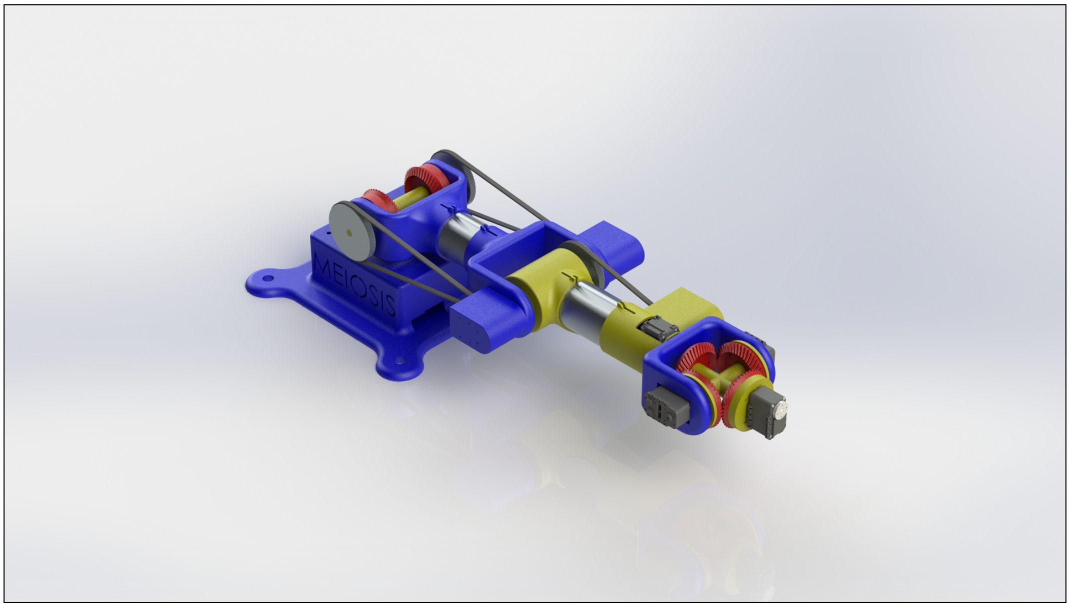


Figure 12: meiosis_zeroed

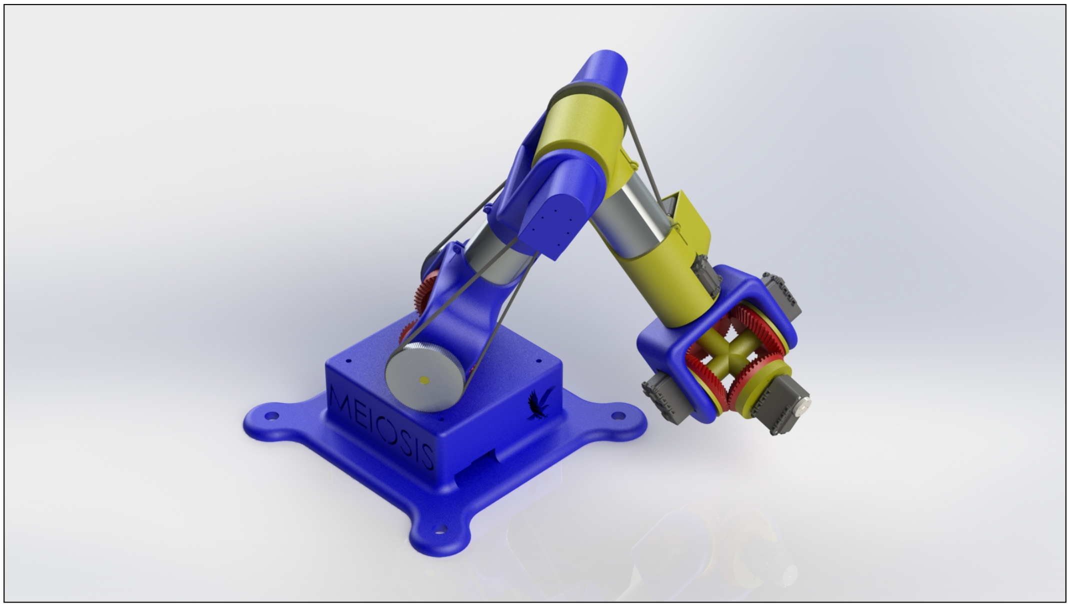


Figure 13: meiosis

### 5.1.1 Pulleys

A 12 tooth and 120 tooth pulleys provide a 10:1 gear ratio and use a 0.25 in wide MXL belt. The center distance between the pulleys must be at least 5.43 in to have 5 teeth meshing. Because of the high gear ratio, greater distances do not increase the number of teeth in mesh. *Figure 14* shows the distance between the manipulator's first two pulleys is 235.185 mm or 9.259 in, which corresponds to a belt with 300 and pitch diameter of 24 in.

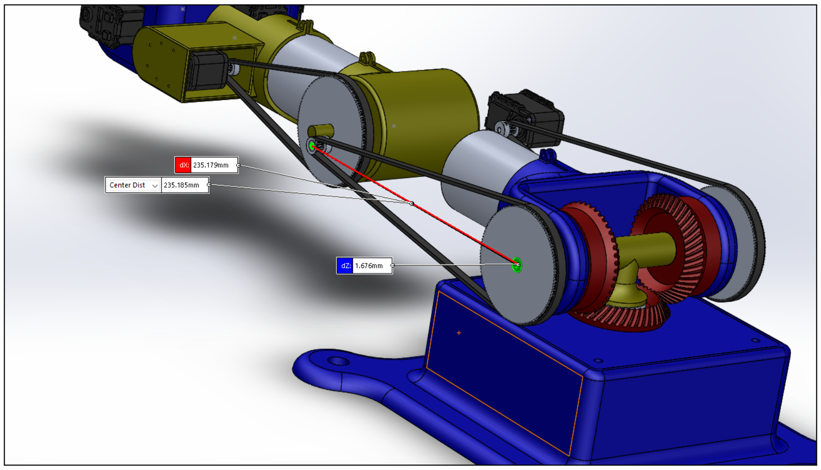


Figure 14: Pulley 1-2 Center Distance

*Figure 15* shows the center distance between the second pulleys is 139.960 mm or 5.510 in. The corresponding belt has 208 teeth with a 16.6 in pitch diameter.

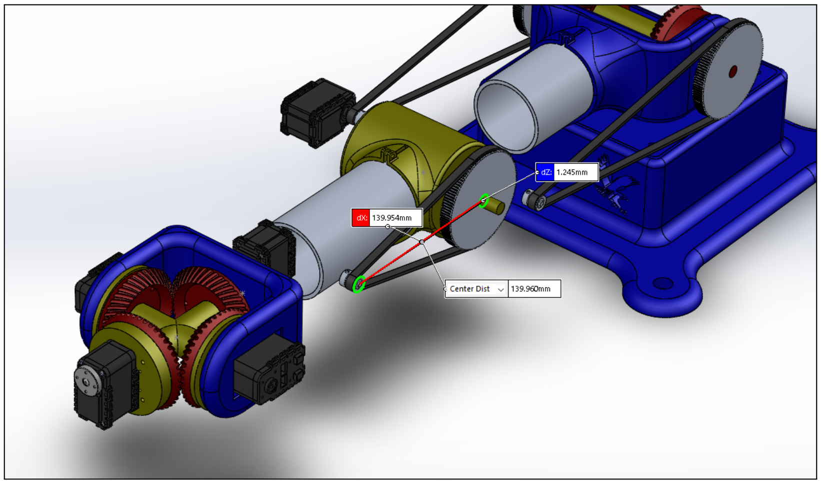


Figure 15: Pulley 3 Center Distance

## 5.2 Forward Kinematics

The forward kinematics of the manipulator are described by the equations below, where the reference coordinate frames are given by *Figure 16*.

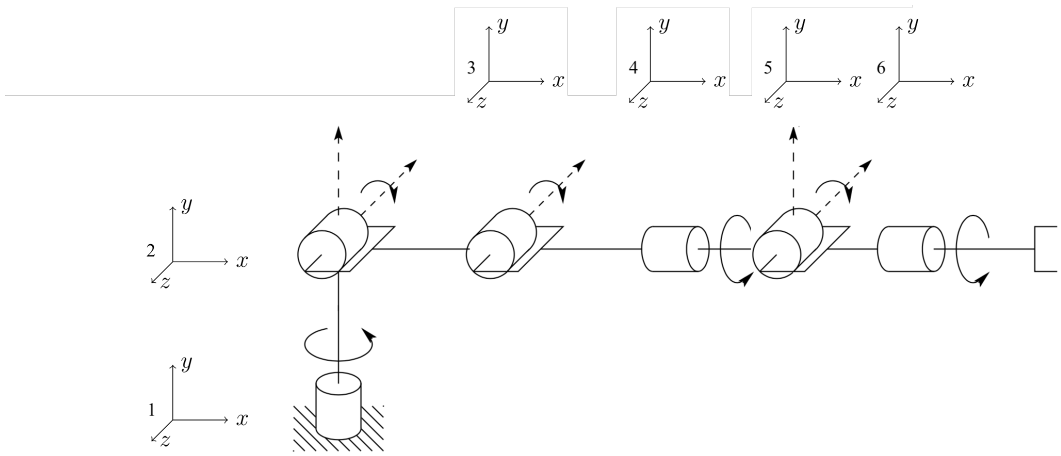


Figure 16: Coordinate Systems

Given the lengths of each of the manipulator links,

$$
{}^I_B r_1 = \begin{bmatrix} 0 \\ 0 \\ \ell_b \end{bmatrix} \quad {}^1_1 r_2 = \begin{bmatrix} 0 \\ 0 \\ \ell_1 \end{bmatrix} \quad {}^2_2 r_3 = \begin{bmatrix} 0 \\ \ell_2 \\ 0 \end{bmatrix} \quad {}^3_3 r_4 = \begin{bmatrix} 0 \\ \ell_3 \\ 0 \end{bmatrix} \quad {}^4_4 r_5 = \begin{bmatrix} 0 \\ \ell_4 \\ 0 \end{bmatrix} \quad {}^5_5 r_6 = \begin{bmatrix} 0 \\ \ell_5 \\ 0 \end{bmatrix}
$$

The position of each link relative to the inertial frame is given as:

$$
\begin{array}{lll}
{}^I_B r_1 = {}_B r_1 & {}^I_B r_2 = r_1 + {}^I T_1 {}^1_1 r_2 & {}^I_B r_3 = r_2 + {}^I T_2 {}^2_2 r_3 \\
{}^I_B r_4 = r_3 + {}^I T_3 {}^3_3 r_4 & {}^I_B r_5 = r_4 + {}^I T_4 {}^4_4 r_5 & {}^I_B r_6 = r_5 + {}^I T_5 {}^5_5 r_6
\end{array}
$$

$$
{}^I_B r_1 = \begin{bmatrix} 0 \\ 0 \\ \ell_b \end{bmatrix} \quad {}^I_B r_2 = \begin{bmatrix} 0 \\ 0 \\ \ell_b + \ell_1 \end{bmatrix} \quad {}^I_B r_3 = \begin{bmatrix} -\ell_2 c_{\theta_2} s_{\theta_1} \\ \ell_2 c_{\theta_{12}} \\ \ell_b + \ell_1 + \ell_2 s_{\theta_2} \end{bmatrix} \quad {}^I_B r_4 = \begin{bmatrix} -s_{\theta_1}(\ell_3 c_{\theta_{23}} + \ell_2 c_{\theta_2}) \\ c_{\theta_1}(\ell_3 c_{\theta_{23}} + \ell_2 c_{\theta_2}) \\ \ell_1 + \ell_b + \ell_3 s_{\theta_{23}} + \ell_2 s_{\theta_2} \end{bmatrix}
$$

$$
{}^I_B r_5 = \begin{bmatrix} -s_{\theta_1}(\ell_3 c_{\theta_{23}} + \ell_4 c_{\theta_{23}} + \ell_2 c_{\theta_2}) \\ c_{\theta_1}(\ell_3 c_{\theta_{23}} + \ell_4 c_{\theta_{23}} + \ell_2 c_{\theta_2}) \\ \ell_1 + \ell_b + \ell_3 s_{\theta_{23}} + \ell_4 s_{\theta_{23}} + \ell_2 s_{\theta_2} \end{bmatrix}
$$

$$
{}^I_B r_6 = \begin{bmatrix} \ell_5 c_{\theta_1} s_{\theta_4} s_{\theta_5} - \ell_4 c_{\theta_{23}} s_{\theta_1} - \ell_2 c_{\theta_2} s_{\theta_1} - \ell_5 c_{\theta_{23}} c_{\theta_5} s_{\theta_1} - \ell_3 c_{\theta_{23}} s_{\theta_1} \\ \quad + \ell_5 c_{\theta_2} c_{\theta_4} s_{\theta_1} s_{\theta_3} s_{\theta_5} + \ell_5 c_{\theta_3} c_{\theta_4} s_{\theta_1} s_{\theta_2} s_{\theta_5} \\ \ell_5(s_{\theta_5}(s_{\theta_1} s_{\theta_4} - c_{\theta_4}(c_{\theta_1} c_{\theta_2} s_{\theta_3} + c_{\theta_1} c_{\theta_3} s_{\theta_2})) - c_{\theta_5}(c_{\theta_1} s_{\theta_2} s_{\theta_3} - c_{\theta_1} c_{\theta_2} c_{\theta_3})) \\ \quad - \ell_3(c_{\theta_1} s_{\theta_2} s_{\theta_3} - c_{\theta_1} c_{\theta_2} c_{\theta_3}) - \ell_4(c_{\theta_1} s_{\theta_2} s_{\theta_3} - c_{\theta_1} c_{\theta_2} c_{\theta_3}) + \ell_2 c_{\theta_1} c_{\theta_2} \\ \ell_1 + \ell_b + \ell_3 s_{\theta_{23}} + \ell_4 s_{\theta_{23}} + \ell_2 s_{\theta_2} + \dfrac{\ell_5 c_{\theta_{23}} s_{\theta_{45}}}{2} + \ell_5 s_{\theta_{23}} c_{\theta_5} - \dfrac{\ell_5 s_{\theta_4 - \theta_5} c_{\theta_{23}}}{2} \end{bmatrix}
$$

Given the direction cosine matrices,

$$rotx(\theta) = \begin{bmatrix} 1 & 0 & 0 \\ 0 & \cos(\theta) & -\sin(\theta) \\ 0 & \sin(\theta) & \cos(\theta) \end{bmatrix} \quad , \quad roty(\theta) = \begin{bmatrix} 1 & 0 & 0 \\ 0 & \cos(\theta) & -\sin(\theta) \\ 0 & \sin(\theta) & \cos(\theta) \end{bmatrix}$$

$$rotz(\theta) = \begin{bmatrix} \cos(\theta) & 0 & \sin(\theta) \\ 0 & 1 & 0 \\ -\sin(\theta) & \cos(\theta) & 0 \end{bmatrix}$$

The orientation of each link with respect to the inertial frame is given as:

$$\begin{aligned}
{}^I T_1 &= rotz(\theta_1) \\
{}^I T_2 &= rotz(\theta_1)\ rotx(\theta_2) \\
{}^I T_3 &= rotz(\theta_1)\ rotx(\theta_2)\ rotx(\theta_3) \\
{}^I T_4 &= rotz(\theta_1)\ rotx(\theta_2)\ rotx(\theta_3)\ roty(\theta_4) \\
{}^I T_5 &= rotz(\theta_1)\ rotx(\theta_2)\ rotx(\theta_3)\ roty(\theta_4)\ rotx(\theta_5) \\
{}^I T_6 &= rotz(\theta_1)\ rotx(\theta_2)\ rotx(\theta_3)\ roty(\theta_4)\ rotx(\theta_5)\ roty(\theta_6)
\end{aligned}$$

$${}^I T_1 = \begin{bmatrix} c_{\theta_1} & -s_{\theta_1} & 0 \\ s_{\theta_1} & c_{\theta_1} & 0 \\ 0 & 0 & 1 \end{bmatrix} \quad {}^I T_2 = \begin{bmatrix} c_{\theta_1} & -c_{\theta_2} s_{\theta_1} & s_{\theta_1} s_{\theta_2} \\ s_{\theta_1} & c_{\theta_1} c_{\theta_2} & -c_{\theta_1} s_{\theta_2} \\ 0 & s_{\theta_2} & c_{\theta_2} \end{bmatrix} \quad {}^I T_3 = \begin{bmatrix} c_{\theta_1} & -c_{\theta_{23}} s_{\theta_1} & s_{\theta_{23}} s_{\theta_1} \\ s_{\theta_1} & c_{\theta_{23}} c_{\theta_1} & -s_{\theta_{23}} c_{\theta_1} \\ 0 & s_{\theta_{23}} & c_{\theta_{23}} \end{bmatrix}$$

$${}^I T_4 = \begin{bmatrix} c_{\theta_1} c_{\theta_4} - s_{\theta_{23}} s_{\theta_1} s_{\theta_4} & -c_{\theta_{23}} s_{\theta_1} & c_{\theta_1} s_{\theta_4} + s_{\theta_{23}} c_{\theta_4} s_{\theta_1} \\ c_{\theta_4} s_{\theta_1} + s_{\theta_{23}} c_{\theta_1} s_{\theta_4} & c_{\theta_{23}} c_{\theta_1} & s_{\theta_1} s_{\theta_4} - s_{\theta_{23}} c_{\theta_1} c_{\theta_4} \\ -c_{\theta_{23}} s_{\theta_4} & s_{\theta_{23}} & c_{\theta_{23}} c_{\theta_4} \end{bmatrix}$$

$${}^I T_5 = \begin{bmatrix} c_{\theta_1} c_{\theta_4} - s_{\theta_{23}} s_{\theta_1} s_{\theta_4} & s_{\theta_5}(c_{\theta_1} s_{\theta_4} + s_{\theta_{23}} c_{\theta_4} s_{\theta_1}) - c_{\theta_{23}} c_{\theta_5} s_{\theta_1} & c_{\theta_5}(c_{\theta_1} s_{\theta_4} + s_{\theta_{23}} c_{\theta_4} s_{\theta_1}) + c_{\theta_{23}} s_{\theta_1} s_{\theta_5} \\ c_{\theta_4} s_{\theta_1} + s_{\theta_{23}} c_{\theta_1} s_{\theta_4} & s_{\theta_5}(s_{\theta_1} s_{\theta_4} - s_{\theta_{23}} c_{\theta_1} c_{\theta_4}) + c_{\theta_{23}} c_{\theta_1} c_{\theta_5} & c_{\theta_5}(s_{\theta_1} s_{\theta_4} - s_{\theta_{23}} c_{\theta_1} c_{\theta_4}) - c_{\theta_{23}} c_{\theta_1} s_{\theta_5} \\ -c_{\theta_{23}} s_{\theta_4} & s_{\theta_{23}} c_{\theta_5} + c_{\theta_{23}} c_{\theta_4} s_{\theta_5} & c_{\theta_{23}} c_{\theta_4} c_{\theta_5} - s_{\theta_{23}} s_{\theta_5} \end{bmatrix}$$

$${}^I T_6 = \begin{bmatrix} {}^I T_{6(1,1)} & {}^I T_{6(1,2)} & {}^I T_{6(1,3)} \\ {}^I T_{6(2,1)} & {}^I T_{6(2,2)} & {}^I T_{6(2,3)} \\ {}^I T_{6(3,1)} & {}^I T_{6(3,2)} & {}^I T_{6(3,3)} \end{bmatrix}$$

$$\begin{aligned}
{}^I T_{6(1,1)} &= c_{\theta_6}(c_{\theta_1} c_{\theta_4} - s_{\theta_{23}} s_{\theta_1} s_{\theta_4}) - s_{\theta_6}(c_{\theta_5}(c_{\theta_1} s_{\theta_4} + s_{\theta_{23}} c_{\theta_4} s_{\theta_1}) + c_{\theta_{23}} s_{\theta_1} s_{\theta_5}) \\
{}^I T_{6(1,2)} &= s_{\theta_5}(c_{\theta_1} s_{\theta_4} + s_{\theta_{23}} c_{\theta_4} s_{\theta_1}) - c_{\theta_{23}} c_{\theta_5} s_{\theta_1} \\
{}^I T_{6(1,3)} &= c_{\theta_6}(c_{\theta_5}(c_{\theta_1} s_{\theta_4} + s_{\theta_{23}} c_{\theta_4} s_{\theta_1}) + c_{\theta_{23}} s_{\theta_1} s_{\theta_5}) + s_{\theta_6}(c_{\theta_1} c_{\theta_4} - s_{\theta_{23}} s_{\theta_1} s_{\theta_4}) \\
{}^I T_{6(2,1)} &= c_{\theta_6}(c_{\theta_4} s_{\theta_1} + s_{\theta_{23}} c_{\theta_1} s_{\theta_4}) - s_{\theta_6}(c_{\theta_5}(s_{\theta_1} s_{\theta_4} - s_{\theta_{23}} c_{\theta_1} c_{\theta_4}) - c_{\theta_{23}} c_{\theta_1} s_{\theta_5}) \\
{}^I T_{6(2,2)} &= s_{\theta_5}(s_{\theta_1} s_{\theta_4} - s_{\theta_{23}} c_{\theta_1} c_{\theta_4}) + c_{\theta_{23}} c_{\theta_1} c_{\theta_5} \\
{}^I T_{6(2,3)} &= s_{\theta_6}(c_{\theta_4} s_{\theta_1} + s_{\theta_{23}} c_{\theta_1} s_{\theta_4}) + c_{\theta_6}(c_{\theta_5}(s_{\theta_1} s_{\theta_4} - s_{\theta_{23}} c_{\theta_1} c_{\theta_4}) - c_{\theta_{23}} c_{\theta_1} s_{\theta_5}) \\
{}^I T_{6(3,1)} &= s_{\theta_6}(s_{\theta_{23}} s_{\theta_5} - c_{\theta_{23}} c_{\theta_4} c_{\theta_5}) - c_{\theta_{23}} c_{\theta_6} s_{\theta_4} \\
{}^I T_{6(3,2)} &= s_{\theta_{23}} c_{\theta_5} + c_{\theta_{23}} c_{\theta_4} s_{\theta_5} \\
{}^I T_{6(3,3)} &= c_{\theta_6}(s_{\theta_{23}} s_{\theta_5} - c_{\theta_{23}} c_{\theta_4} c_{\theta_5}) - c_{\theta_{23}} s_{\theta_4} s_{\theta_6}
\end{aligned}$$

## 5.3 Velocity Kinematics

The translational and rotational velocties ($\dot{r}$ & $\omega$) can be found given the geometric jacobian of the body and transformation matrix corresponding to it.

$$\begin{bmatrix} {}^B_B\omega_I \\ {}^I_B\dot{r}_B \end{bmatrix} = J_B = \begin{bmatrix} {}^IT_B(:,3)^T \cdot \dfrac{\partial}{\partial\gamma}{}^IT_B(:,2) \\ {}^IT_B(:,1)^T \cdot \dfrac{\partial}{\partial\gamma}{}^IT_B(:,3) \\ {}^IT_B(:,2)^T \cdot \dfrac{\partial}{\partial\gamma}{}^IT_B(:,1) \end{bmatrix}$$

## 5.4 Inverse Kinematics

The inverse kinematics can be calculated given desired position and orientation vectors, $o$ and $R$, respecitvely.

$$\begin{bmatrix} x_c & y_c & z_c \end{bmatrix} = o \ , \quad R = \begin{bmatrix} r_{11} & r_{12} & r_{13} \\ r_{21} & r_{22} & r_{23} \\ r_{31} & r_{32} & r_{33} \end{bmatrix}$$

Inverse Position :

$$\begin{aligned} \theta_1 &= \text{atan2}\left(x_c,\ y_c\right) - {}^{\pi}\!/_{2} \\ \theta_2 &= \text{atan2}\left(z_c - \ell_1,\ \sqrt{x_c^2 + y_c^2}\right) - \text{atan2}\left(\ell_3 s_3,\ \ell_2 + \ell_3 c_3\right) \\ \theta_3 &= \text{atan2}(-\sqrt{1 - D^2},\ D) \\ &\quad \text{where } D \equiv \frac{x_c^2 + y_c^2 + (z_c - \ell_1)^2 - \ell_2^2 - \ell_3^2}{2\ell_2\ell_3} \end{aligned}$$

Inverse Orientation :

$$\begin{aligned} {}^IT_3 &= rotz(\theta_1)\ rotx(\theta_2)\ rotx(\theta_3) \\ {}^3T_6 &= {}^IT_3^T R \\ \theta_4 &= \text{atan2}\left({}^3T_{6(1,2)},\ {}^3T_{6(3,2)}\right) \\ \theta_5 &= \text{atan2}\left({}^3T_{6(3,2)}/c_4,\ {}^3T_{6(2,2)}\right) \\ \theta_6 &= \text{atan2}\left({}^3T_{6(2,1)},\ \ -{}^3T_{6(2,3)}\right) \end{aligned}$$

## 5.5 Equations of Motion

Given robot dynamics described by $H(\gamma)\ddot{\gamma} + d(\gamma,\dot{\gamma}) + G(\gamma) = F_\gamma$, the equations of motion for the manipulator can be determined. Solving this equation for $\ddot{\gamma}$ gives:

$$\ddot{\gamma} = H(\gamma)^{-1}\left(F_\gamma - d(\gamma,\dot{\gamma}) - G(\gamma)\right) \tag{1}$$

Where $F_\gamma$ is the vector of generalized forces on the joints and

$$H(\gamma) = \sum_{B}^{N} J_B(\gamma)^T \begin{bmatrix} {}^B_B J & \mathring{S}({}^B_B\Gamma)^I T_B^T \\ {}^I T_B \mathring{S}({}^B_B\Gamma)^T & m_B I \end{bmatrix} J_B(\gamma)\ , \quad {}^B_B\Gamma =_B^B r_{cm} m_b\ , \quad \mathring{S}(\omega)r = (\omega \times r)$$

$$d(\gamma,\dot{\gamma}) = \sum_{B}^{N} J_B(\gamma)^T \begin{bmatrix} {}^B_B J & \mathring{S}({}^B_B\Gamma)^I T_B^T \\ {}^I T_B \mathring{S}({}^B_B\Gamma)^T & m_B I \end{bmatrix} \dot{J}_B(\gamma,\dot{\gamma})\dot{\gamma} + J_B(\gamma)^T \begin{bmatrix} {}^B_B\omega_I \times^B_B J^B_B\omega_I \\ {}^I T_B \left({}^B_B\omega_I \times ({}^B_B\omega_I \times^B_B \Gamma)\right) \end{bmatrix}$$

$$G(\gamma) = \left(\frac{\partial U({}^I r(\gamma))}{\partial \gamma}\right)^T \ , \quad U_B = \begin{bmatrix} 0 & 0 & g \end{bmatrix} \left({}^I_B r_B m_B +^I T_B {}^B_B\Gamma\right)$$

### 5.5.1 Actuator Dynamics

Given robot dynamics described by $H(\gamma)\ddot{\gamma} + n(\gamma,\dot{\gamma}) = \tau$, the torque, $\tau$, provided by the servo motors is necessary to solve the closed loop dynamics of the system. Assuming the servo is driven by a D.C. motor with proportional derivative control,

$$\tau_a = K i_a = J_a\ddot{\theta}_a + b_a\dot{\theta}_a + \tau_L \tag{2}$$

Where $\tau_a$ is the actuator torque, $K$ is the back-EMF constant, $i_a$ is the motor current, $J_a$ is the armature inertia, $\theta_a$, $\dot{\theta}_a, \ddot{\theta}_a$ is the motor position and it's first and second time derivatives respectively, $b_a$ is the viscous friction coefficient, and $\tau_L$ is the torque available for the actuator to do work. The basic equation for a motor is known to be:

$$V_a = i_a R_a + K\dot{\theta}_a \tag{3}$$

Where $V_a$ is the voltage applied to the actuator and $R_a$ is the armature resistance. Given a gearbox with in/out ratio $N$ and efficiency $\eta$,

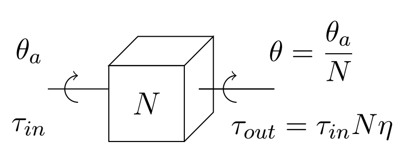


The motor equation (2) can be expressed in the output coordinates:

$$K i_a = J_a N\ddot{\theta} + b_a N\dot{\theta} + \frac{\tau}{N\eta}$$

Substituing into equation (3) and solving for $i_a$:

$$i_a = \frac{J_a N}{K}\ddot{\theta} + b_a N\dot{\theta} + \frac{\tau}{N\eta}$$

$$V_a = \frac{R_a J_a N}{K}\ddot{\theta} + \frac{R_a b_a N}{K}\dot{\theta} + \frac{R_a}{KN\eta}\tau + KN\dot{\theta} \tag{4}$$

Assuming PD control, $V_a = K_p(\theta - \theta_d) + K_d\dot{\theta}$, where $\theta_d$ is the desired orientation of the actuator, the following solution is found by setting the PD solution equal to (4). After collecting like terms:

$$\frac{R_a J_a N}{K}\ddot{\theta} + \left(\frac{R_a J_a N}{K} - K_d + KN\right)\dot{\theta} - K_p\theta = -K_p\theta_d - \frac{R_a}{KN\eta}\tau \tag{5}$$

The following parameters of the system can be obtained by applying a step input to the system with $\tau = 0$ and measuring the characteristics of it's response. Denoting $\zeta$ as the damping ratio and $\omega_n$ as the natural frequency of the system,

$$\%\text{ Overshoot} = \left(\frac{\theta_{max} - \theta_{ss}}{\theta_{ss}}\right) \times 100 \ , \quad \zeta = \frac{-\ln(\%\text{OS}/100)}{\sqrt{\pi^2 + \ln^2(\%\text{OS}/100)}} \ , \quad \omega_n = \frac{\pi}{T_p\sqrt{1-\zeta^2}}$$

Given $\theta_{max}$, $\theta_{ss}$, and $T_p$ as measured parameters of the system's max output, steady state, and time to peak, respectively.

Refactoring equation (5) and equating with the general solution for a second order system given by $\ddot{\theta} + 2\zeta\omega_n\dot{\theta} + \omega_n^2\theta = \omega_n^2\theta_d$, the following solutions are found:

$$2\zeta\omega_n = \frac{b_a}{J_a} - \frac{KK_d}{R_a J_a N} + \frac{K^2}{R_a J_a} \tag{6}$$

$$\omega_n^2 = \frac{-KK_p}{R_a J_a N} \tag{7}$$

Performing a similar experiment as previously described, except with a known inertial load $\tau = J_m\ddot{\theta}$, the following parameters can be found:

$$\alpha_m \equiv 2\zeta\omega_n = \frac{R_a b_a N^2\eta - KK_d N\eta + K^2N^2\eta}{R_a J_a N^2\eta + R_a J_m} \ , \quad \beta_m \equiv \omega_n = -\frac{KK_p N\eta}{R_a J_a N^2\eta + R_a J_m}$$

$$\begin{bmatrix} 1 & -(\alpha_1 J_1 + \beta_1 J_1) \\ 1 & -(\alpha_2 J_2 + \beta_2 J_2) \\ \vdots & \vdots \end{bmatrix} \begin{bmatrix} \dfrac{R_a b_a N^2\eta - KK_d N\eta + K^2N^2\eta - KK_p N\eta}{R_a J_a N^2\eta} \\ \\ \dfrac{1}{J_a N^2\eta} \end{bmatrix} = \begin{bmatrix} \alpha_1 + \beta_1 \\ \alpha_2 + \beta_2 \\ \vdots \end{bmatrix} \tag{8}$$

With multiple datasets (varying inertial loads, $J_m$), the solutions of (8) can be found using the least-squares method, yeilding

$$\frac{R_a b_a N - KK_d + K^2 N\eta - KK_p}{R_a J_a N} \quad (9) \qquad \frac{1}{J_a N^2 \eta} \quad (10)$$

Finally, the coefficients of the second order system (11) are known:

$$\underbrace{\left(J_a N^2 \eta\right)}_{1/(10)} \ddot{\theta} + \underbrace{\left(\frac{R_a b_a N^2 \eta - KK_d N\eta + K^2 N^2 \eta}{R_a}\right)}_{(6)/(10)} \dot{\theta} - \underbrace{\left(\frac{KK_p N\eta}{R_a}\right)}_{(7)/(10)} \theta + \underbrace{\left(\frac{KK_p N\eta}{R_a}\right)}_{(7)/(10)} \theta_d = -\tau \quad (11)$$

The MATLAB code implementing this process can be found in the Appendix (see section I, p. 34, *Listing 1*). The torque provided by the servo can now be solved for, given the current position ($\theta$), velocity ($\dot{\theta}$), angular acceleration ($\ddot{\theta}$), and desired position ($\theta_d$) are known.

Given the equation of motionfor the dynamical response of the system (1), substituting in the solution obtained for the motor dynamics and solving for the acceleration,

$$\left(H + J_a N^2 \eta\right)^{-1} \left[\left(B - \frac{R_a b_a N^2 \eta - KK_d N\eta + K^2 N^2 \eta}{R_a}\right) \dot{\gamma} - \left(\frac{KK_p N\eta}{R_a}\right)(\gamma_d - \gamma) - n\right] = \ddot{\gamma} \quad (12)$$

Where

$$n(\gamma, \dot{\gamma}) = d(\gamma, \dot{\gamma}) + G(\gamma) + C\mathrm{sgn}(\dot{\gamma})$$

## 5.6 Open-Loop Simulation

The equations of motion described in equation (1) can be integrated to simulate the motion of the system. For the open loop control, no input torque is supplied, meaning the system responds only to gravity. Due to the complexity of the equations of motion, they will be integrated numerically using a 4th Order Runge Kutta algorithm. Since so input force is supplied, the equations of motion reduce down to the relation described in equation (13).

$$\ddot{\gamma} = H(\gamma)^{-1}(-d(\gamma, \dot{\gamma}) - G(\gamma)) \quad (13)$$

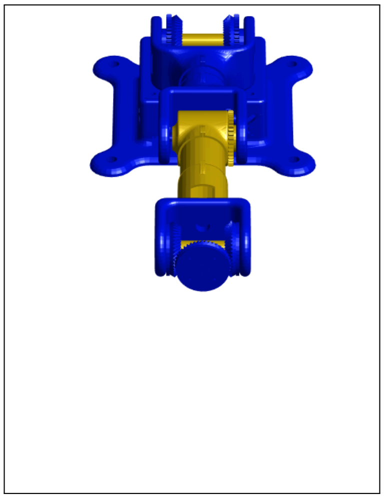

(a) Frame Snapshot near Simulation Initiation

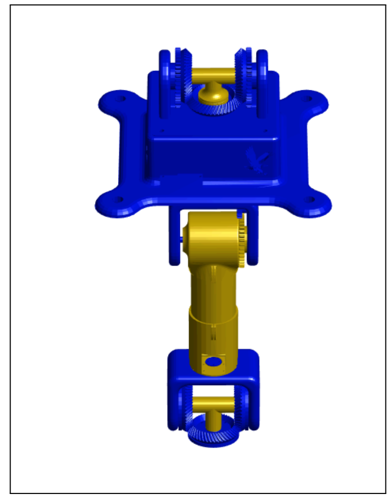

(b) Frame Snapshot near Simulation Termination

Figure 17: Open-Loop Control Simulation Animation Snapshots

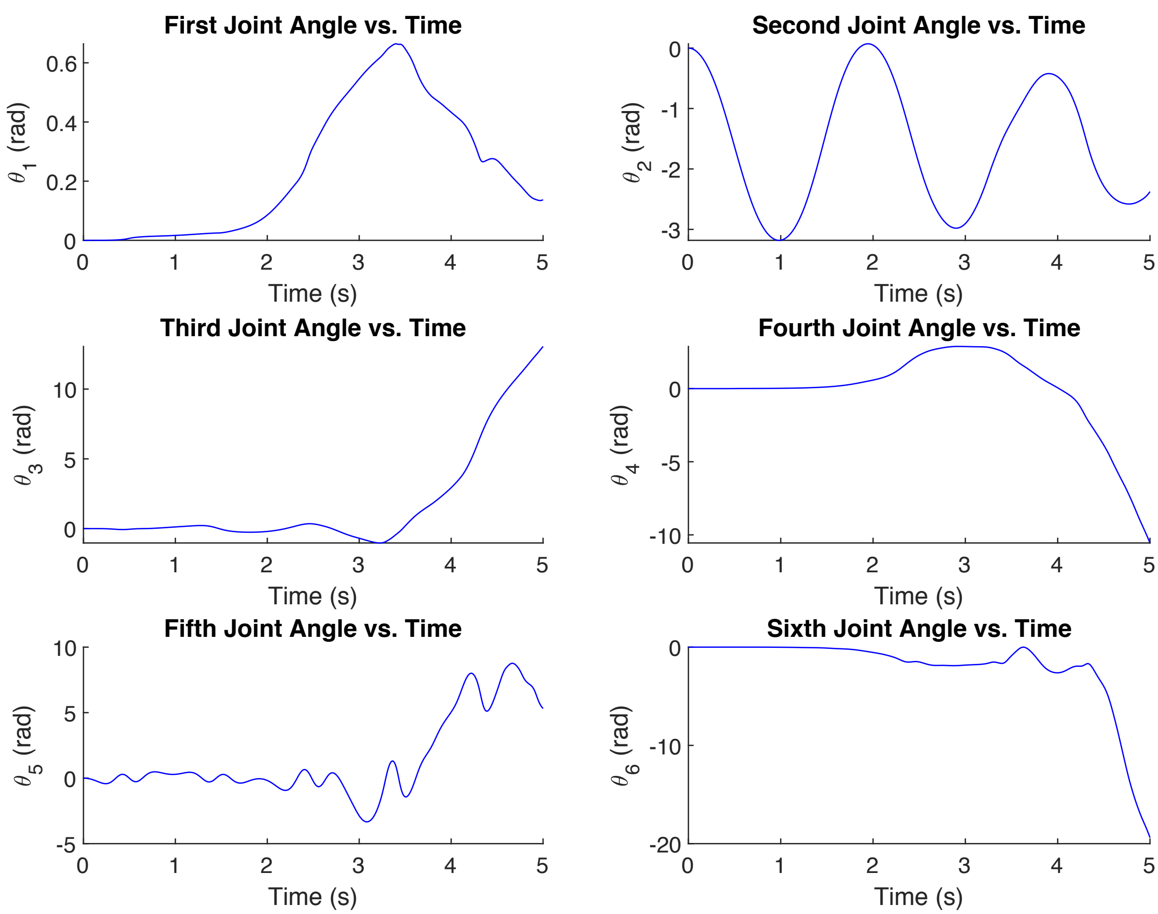


Figure 18: Joint Angles vs Time in Open-Loop Simulation

## 5.7 Control System

## 5.8 Closed-Loop Simulation

The motor equation (11) gives an expression for the motor torques, however the system dynamics are defined in terms of geometric joint angles. The inclusion of differential drive systems means that the joint angles, $\gamma$ do not directly correspond to motor rotations, $\theta$. However, there is a linear relation between them, described in equation (14).

$$\gamma = A \cdot \theta \quad \text{where} \quad A = \begin{bmatrix} 1/(2N) & 1/(2N) & 0 & 0 & 0 & 0 \\ 1/(2N) & -1/(2N) & 0 & 0 & 0 & 0 \\ 0 & 0 & -1/N & 0 & 0 & 0 \\ 0 & 0 & 0 & 1 & 0 & 0 \\ 0 & 0 & 0 & 0 & -1/2 & 1/2 \\ 0 & 0 & 0 & 0 & 1/2 & 1/2 \end{bmatrix} \tag{14}$$

Equation (14) can be used to map the joint angles to the motor angles. The gear ratio of 1:10 is represented by the variable N. Similarly, the motor angles can be determined by multiplying both sides of equation (14) by the inverse of matrix A, giving the following relation.

$$\theta = A^{-1}\gamma \tag{15}$$

It is important to note that the virtual work done by the joint torques ($F_\gamma$) and the virtual work done by the motor torques ($F_\theta$) are equal. Using equation (15), a linear relation between the joint torques and motor torques can be determined.

$$\begin{aligned} \delta W = F_\theta^T \delta\theta &= F_\gamma^T \delta\gamma, \text{ where } \delta\gamma = A\delta\theta \\ F_\theta^T \delta\theta &= F_\gamma^T (A\delta\theta) \\ F_\theta^T &= F_\gamma^T A \\ \left(F_\theta^T\right)^T &= \left(F_\gamma^T A\right)^T \\ F_\theta = A^T F_\gamma &\Leftrightarrow F_\gamma = A^{-T} F_\theta \end{aligned}$$

Using this equation, a relation can be determined between the motor dynamics and the system dynamics given in equation (11) and equation (1) respectively.

$$H(\gamma)\ddot{\gamma} + d(\gamma,\dot{\gamma}) + G(\gamma) = -A^{-T}\left(C_1 A^{-1}\ddot{\gamma} + C_2 A^{-1}\dot{\gamma} + C_3\theta_d - C_3 A^{-1}\gamma\right)$$

$$\ddot{\gamma} = H(\gamma)^{-1}\left(-A^{-T}\left(C_1 A^{-1}\ddot{\gamma} + C_2 A^{-1}\dot{\gamma} + C_3\theta_d - C_3 A^{-1}\gamma\right) - d(\gamma,\dot{\gamma}) - G(\gamma)\right) \tag{16}$$

Because this equation includes the motor model, which in turn includes an internal PD controller, this equation can be integrated to solve for the system response given a desired motor angle input, $\theta_d$. However, doing so will not result in the desired system response. This control scheme does not have any compensation for the inertia of the links, and it is also lacking gravity compensation. This can be remedied by modifying the input to the motors, $\theta_d$. A new input, $u$, is defined such that gravity can be compensated. Thus, the motor input term in equation (16) must include both compensation for gravity and the desired motor angle.

$$A^{-T}C_3u = G(\gamma) + d(\gamma,\dot{\gamma}) + A^{-T}C_3\theta_d$$

$$u = \left(A^{-T}C_3\right)^{-1} G(\gamma) + \theta_d \tag{17}$$

With this new motor input, the closed loop control system equations of motion are given as:

$$\ddot{\gamma} = H(\gamma)^{-1}\left(-A^{-T}\left(C_1A^{-1}\ddot{\gamma} + C_2A^{-1}\dot{\gamma} + C_3u - C_3A^{-1}\gamma\right) - d(\gamma,\dot{\gamma}) - G(\gamma)\right) \tag{18}$$

Equation (18) can then be integrated to solve for the system response given desired motor angles.

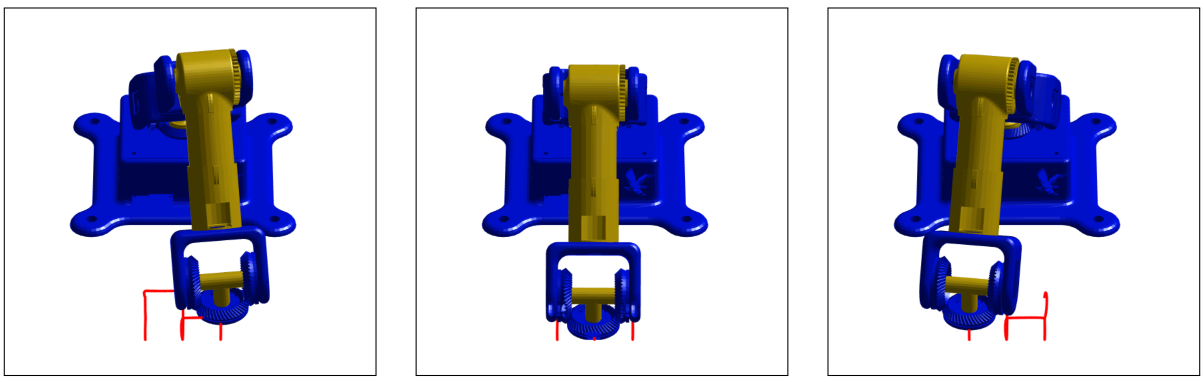

(a) Frame Snapshot near Simulation Initiation

(b) Frame Snapshot near Simulation Middle

(c) Frame Snapshot near Simulation Termination

Figure 19: Closed-Loop Control Simulation Animation Snapshots

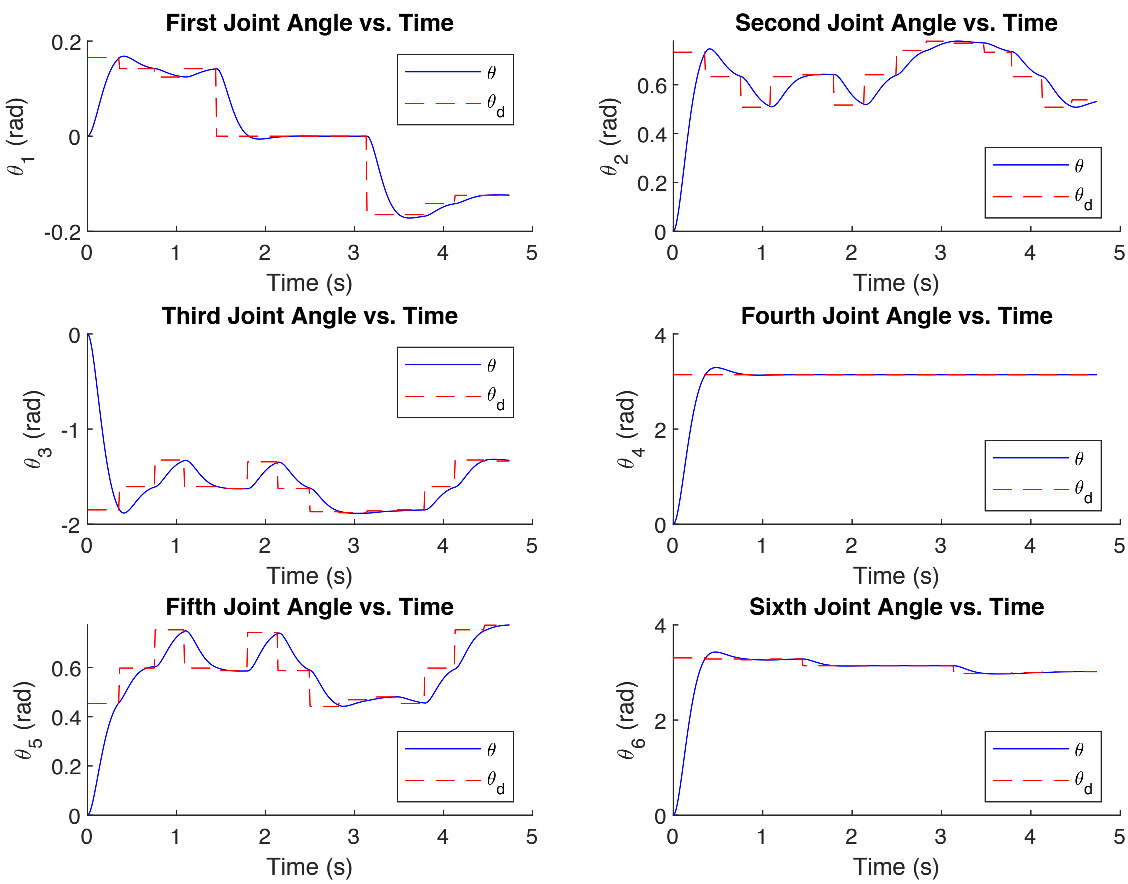


Figure 20: Joint Angles vs Time in Closed-Loop Simulation

## 5.9 ANSYS

## 5.10 Electrical Schematic

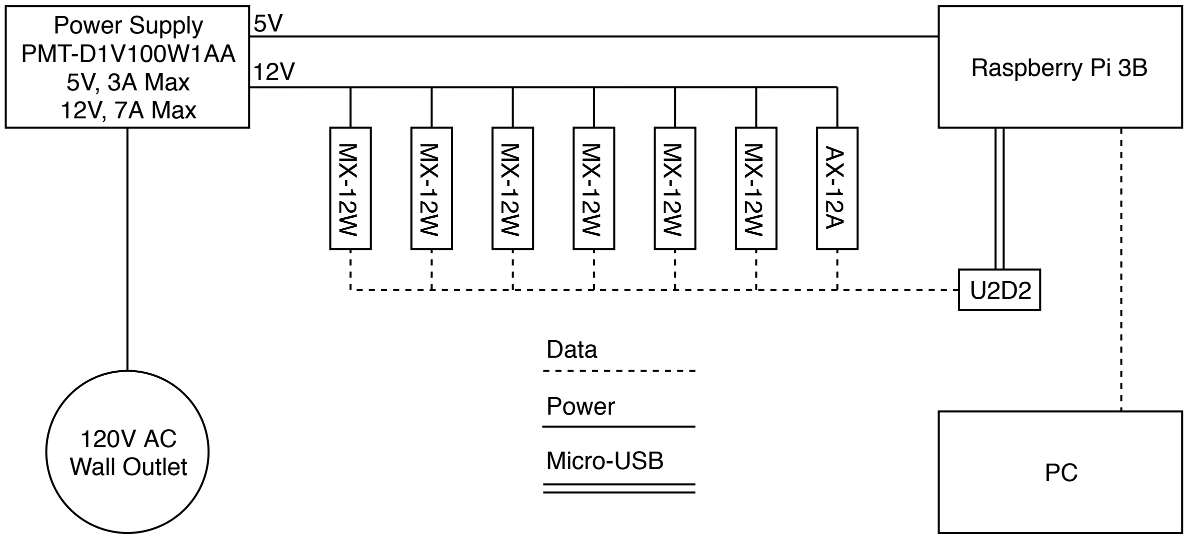


Figure 21: Electrical Schematic

### 5.11 Software Flowchart

### 5.12 Project Status and Future

### 5.13 Parts List

## Acknowledgements & Attributions

We would like to acknowledge the following people for their contibutions in creating this report**?**

— Dr. Isenberg

— Dr. Schipper

# References


[1] S. Hutchinson M. Spong and M. Vidyasager. *Robot Modeling and Control*. 2006.

# I Appendix

## i Relevant Figures and Materials

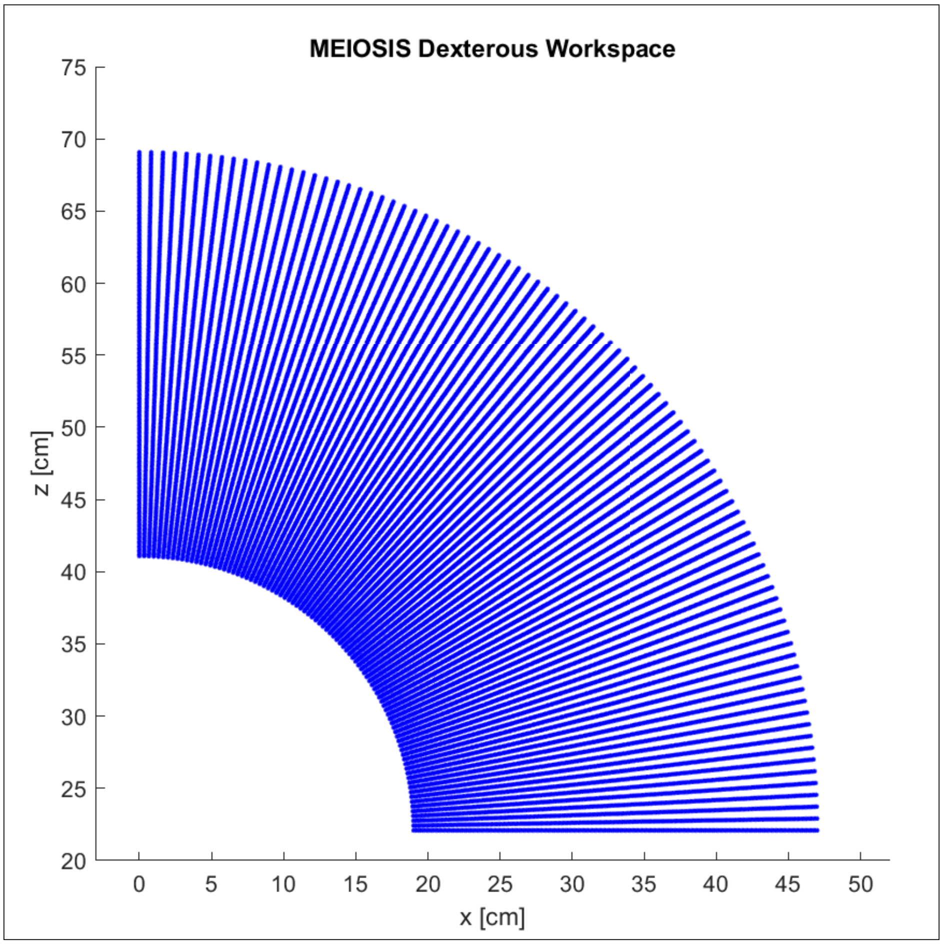


Figure 22: Cross Section of Dexterous Workspace Quadrant

## ii CAD Drawings

The complete drawing package is attached.

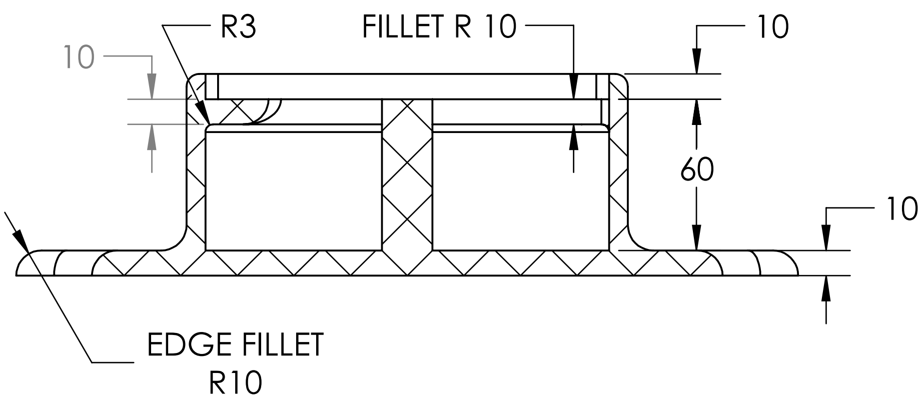


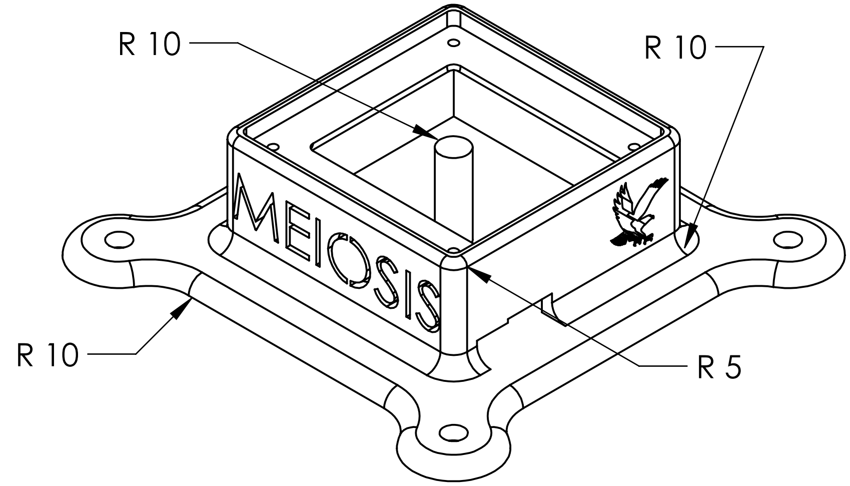


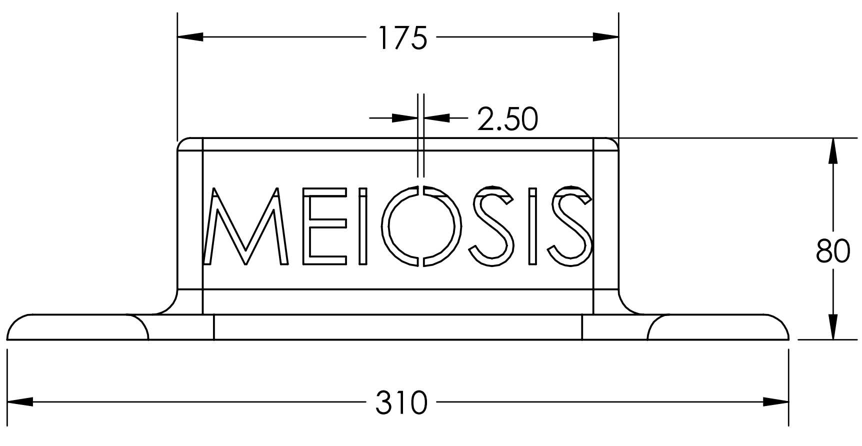


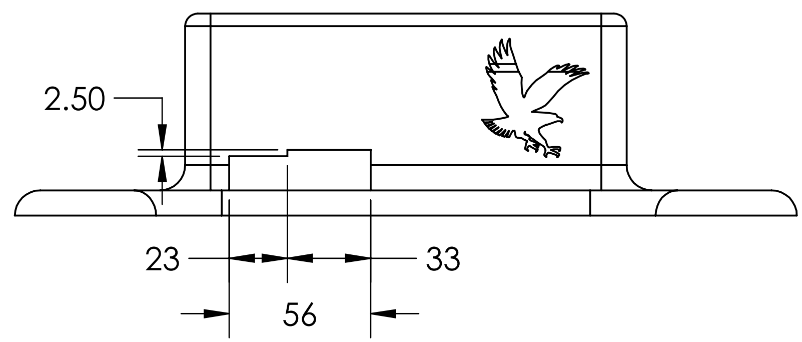


| UNLESS OTHERWISE SPECIFIED: | | NAME | DATE | |
|---|---|---|---|---|
| DIMENSIONS ARE IN MILLIMETERS | DRAWN | Ryan W. | 11/13/2019 | TITLE: |
| TOLERANCES: ±3.0 | CHECKED | | | Base Bottom |
| | ENG APPR. | | | |
| | MFG APPR. | | | |
| INTERPRET GEOMETRIC TOLERANCING PER: | Q.A. | | | |
| MATERIAL PLA, 30% Infill | COMMENTS: | | | SIZE A / DWG. NO. / REV 1.0 |
| FINISH N/A | | | | |
| DO NOT SCALE DRAWING | | | | SCALE: 1:5 / WEIGHT: / SHEET 1 OF 13 |

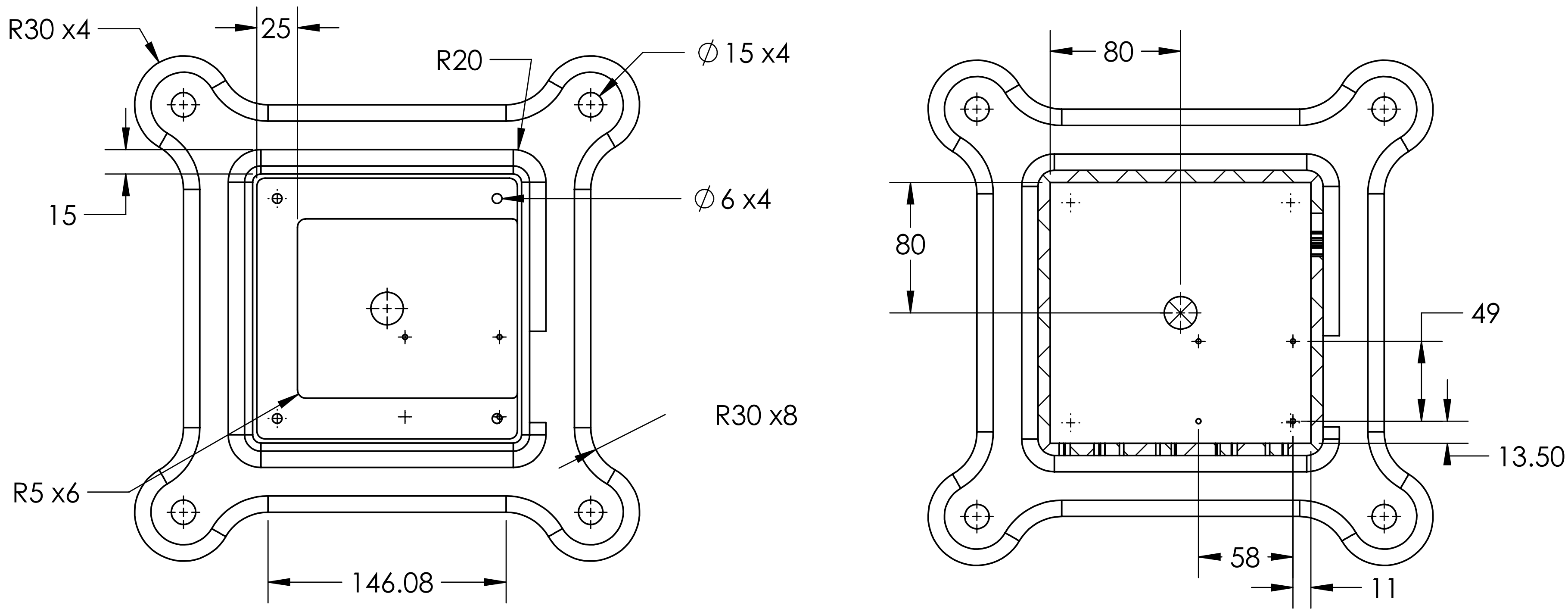


| UNLESS OTHERWISE SPECIFIED: | | NAME | DATE | |
|---|---|---|---|---|
| DIMENSIONS ARE IN MILLIMETERS | DRAWN | Ryan W. | 11/13/2019 | |
| TOLERANCES: ±3.0 | CHECKED | | | TITLE: |
| | ENG APPR. | | | Base Bottom |
| | MFG APPR. | | | |
| INTERPRET GEOMETRIC TOLERANCING PER: | Q.A. | | | |
| MATERIAL: PLA, 30% Infill | COMMENTS: | | | SIZE A / DWG. NO. / REV 1.0 |
| FINISH: N/A | | | | |
| DO NOT SCALE DRAWING | | | | SCALE: 1:5 / WEIGHT: / SHEET 2 OF 13 |

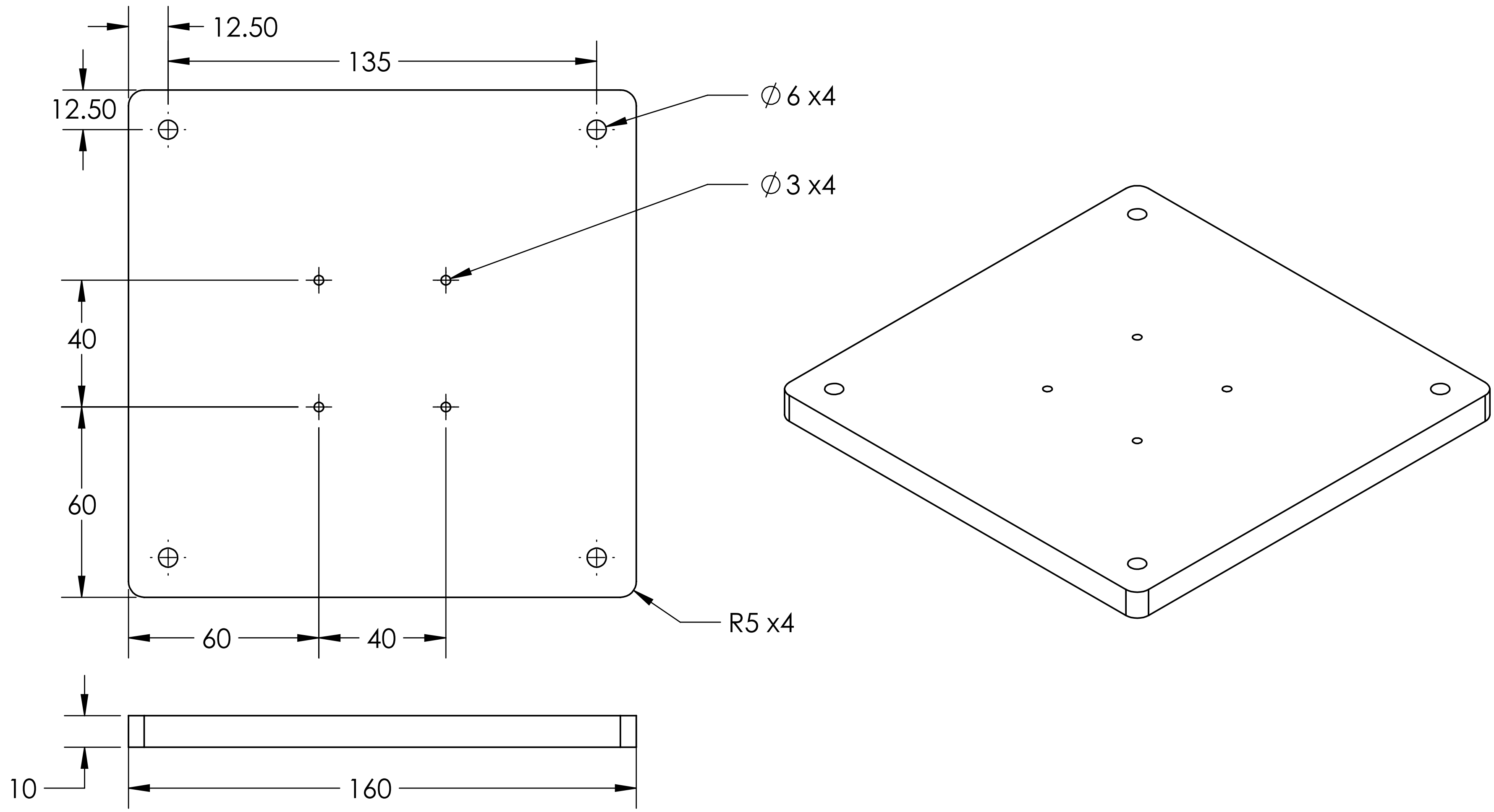


| UNLESS OTHERWISE SPECIFIED: | | NAME | DATE | |
|---|---|---|---|---|
| DIMENSIONS ARE IN MILLIMETERS | DRAWN | Ryan W. | 11/8/2019 | |
| TOLERANCES: ±3.0 | CHECKED | | | TITLE: Base Top |
| | ENG APPR. | | | |
| | MFG APPR. | | | |
| | Q.A. | | | |
| INTERPRET GEOMETRIC TOLERANCING PER: | COMMENTS: | | | SIZE A |
| MATERIAL PLA, 30% Infill | | | | DWG. NO. |
| FINISH N/A | | | | REV 1.0 |
| DO NOT SCALE DRAWING | | | | SCALE: 1:5 WEIGHT: SHEET 3 OF 13 |

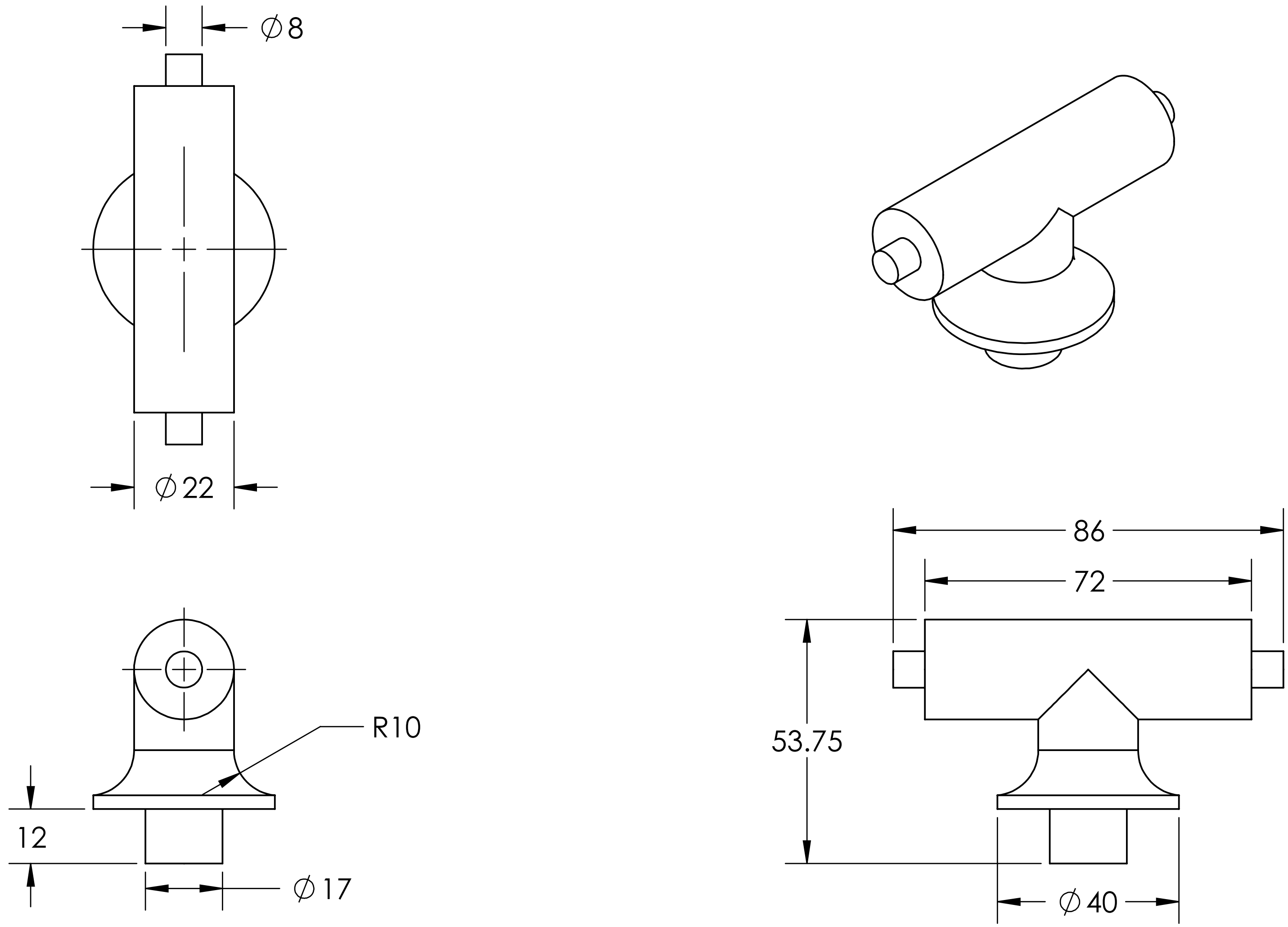


| UNLESS OTHERWISE SPECIFIED: | | NAME | DATE | |
|---|---|---|---|---|
| DIMENSIONS ARE IN MILLIMETERS<br>TOLERANCES: ±3.0 | DRAWN | Ryan W. | 11/8/2019 | TITLE:<br>Shoulder Differential T-Bar |
| | CHECKED | | | |
| | ENG APPR. | | | |
| | MFG APPR. | | | |
| INTERPRET GEOMETRIC TOLERANCING PER: | Q.A. | | | |
| MATERIAL<br>PLA, 30% Infill | COMMENTS: | | | SIZE A / DWG. NO. / REV 1.0 |
| FINISH<br>N/A | | | | |
| DO NOT SCALE DRAWING | | | | SCALE: 1:2 / WEIGHT: / SHEET 4 OF 13 |

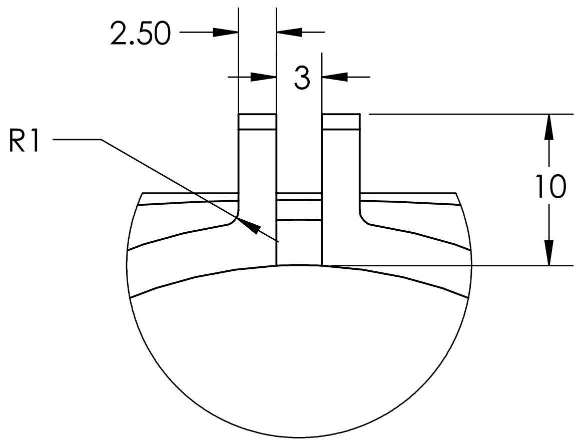


SCALE 2:1

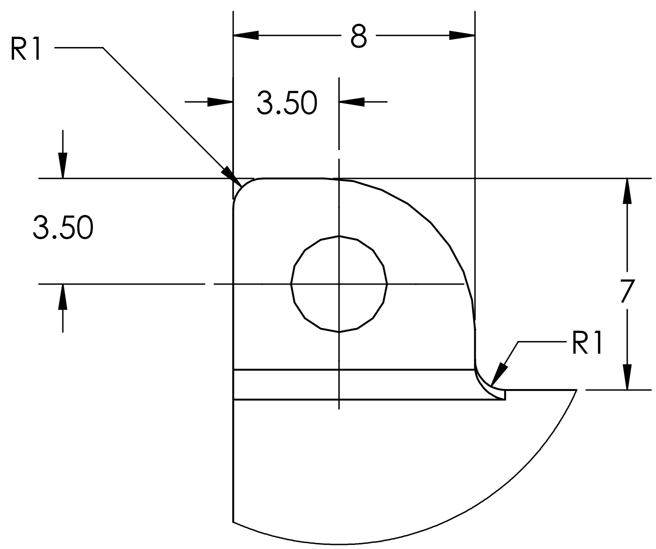


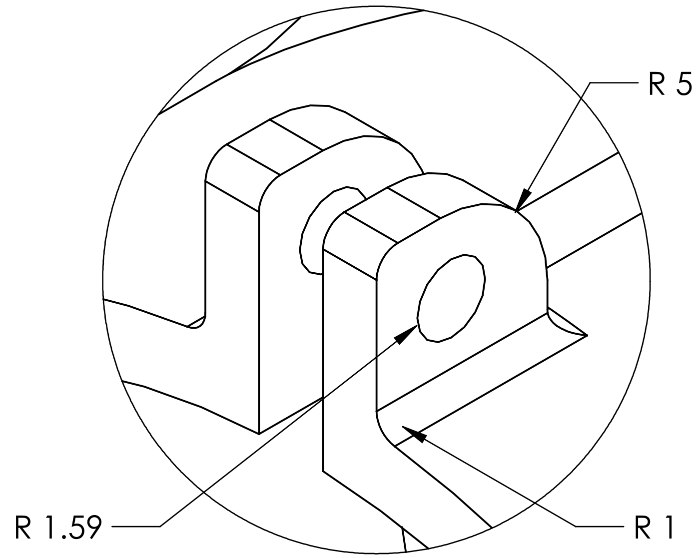


| UNLESS OTHERWISE SPECIFIED: | | NAME | DATE | |
|---|---|---|---|---|
| DIMENSIONS ARE IN MILLIMETERS | DRAWN | Ryan W. | 11/20/2019 | |
| TOLERANCES: ±3.0 | CHECKED | | | TITLE: |
| | ENG APPR. | | | CLAMP DESIGN |
| | MFG APPR. | | | |
| INTERPRET GEOMETRIC TOLERANCING PER: | Q.A. | | | |
| MATERIAL: PLA | COMMENTS: THIS DRAWING SHOWS THE CLAMPING MECHANISM TO BE USED FOR LINK 2_A, LINK 2_B, LINK 3_A, AND LINK 3_B. | | | SIZE: A · DWG. NO. · REV: 1.0 |
| FINISH: N/A | | | | SCALE: 4:1 · WEIGHT: · SHEET 5 OF 13 |
| DO NOT SCALE DRAWING | | | | |

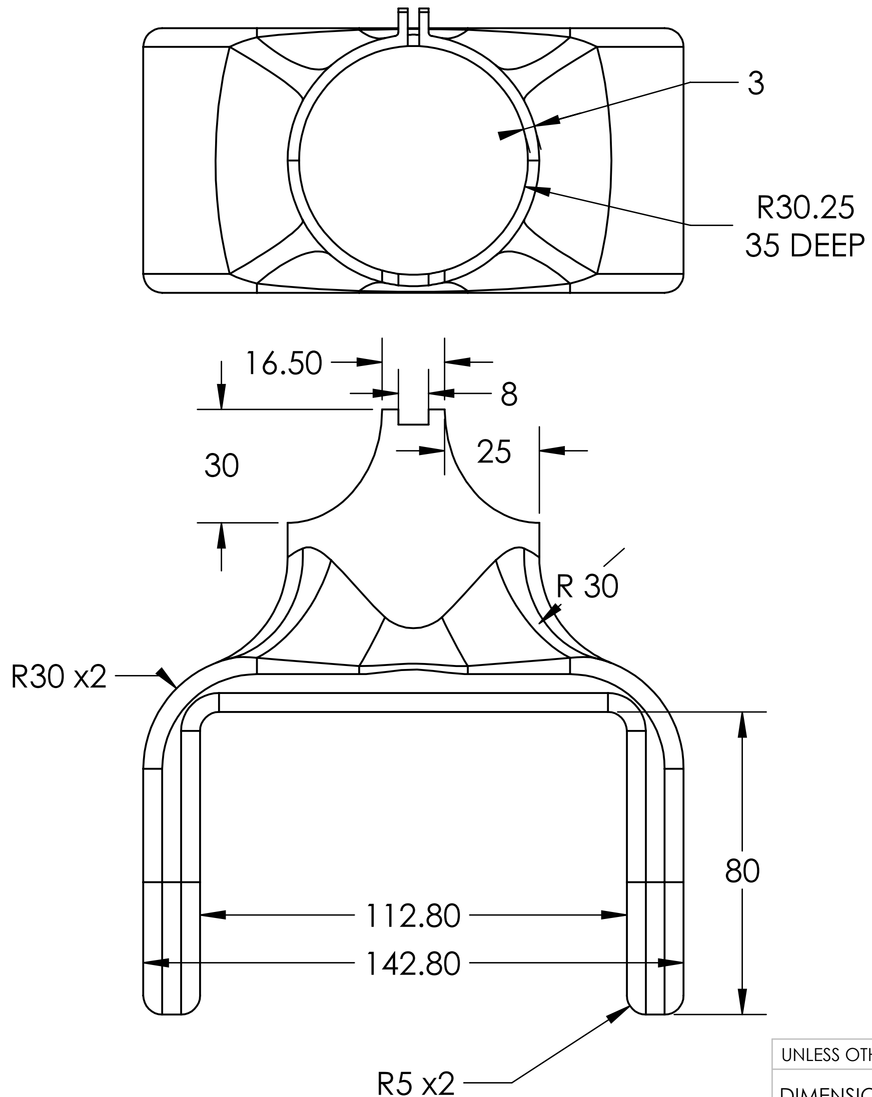


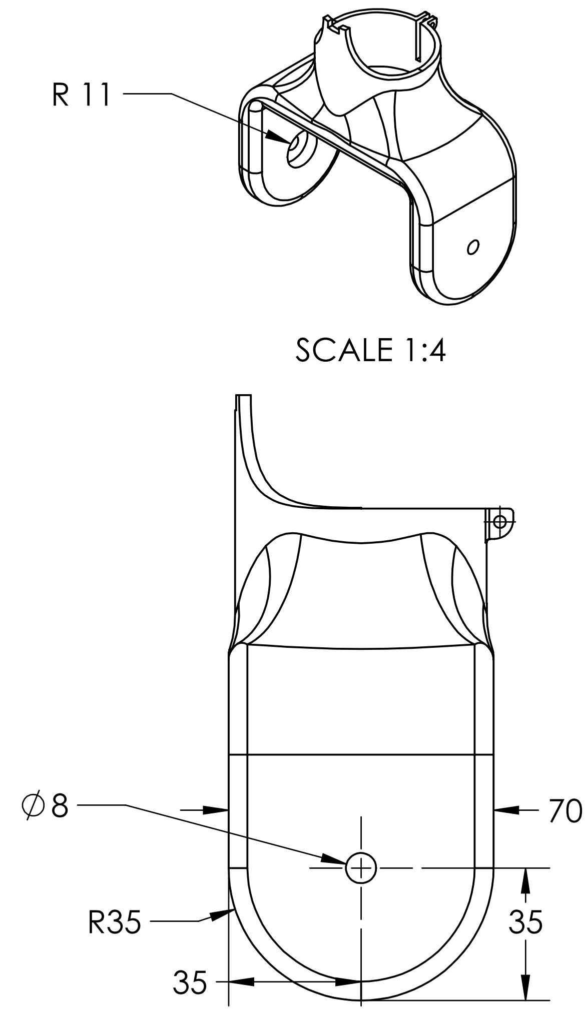


| UNLESS OTHERWISE SPECIFIED: | | NAME | DATE | |
|---|---|---|---|---|
| DIMENSIONS ARE IN MILLIMETERS | DRAWN | Ryan W. | 11/11/2019 | |
| TOLERANCES: ±3.0 | CHECKED | | | TITLE: Link 2_a |
| | ENG APPR. | | | |
| | MFG APPR. | | | |
| INTERPRET GEOMETRIC TOLERANCING PER: | Q.A. | | | |
| MATERIAL: PLA, 30% Infill | COMMENTS: | | | SIZE: A |
| FINISH: N/A | | | | DWG. NO. |
| DO NOT SCALE DRAWING | | | | REV 1.0 |
| | | | | SCALE: 1:2 |
| | | | | WEIGHT: |
| | | | | SHEET 6 OF 13 |

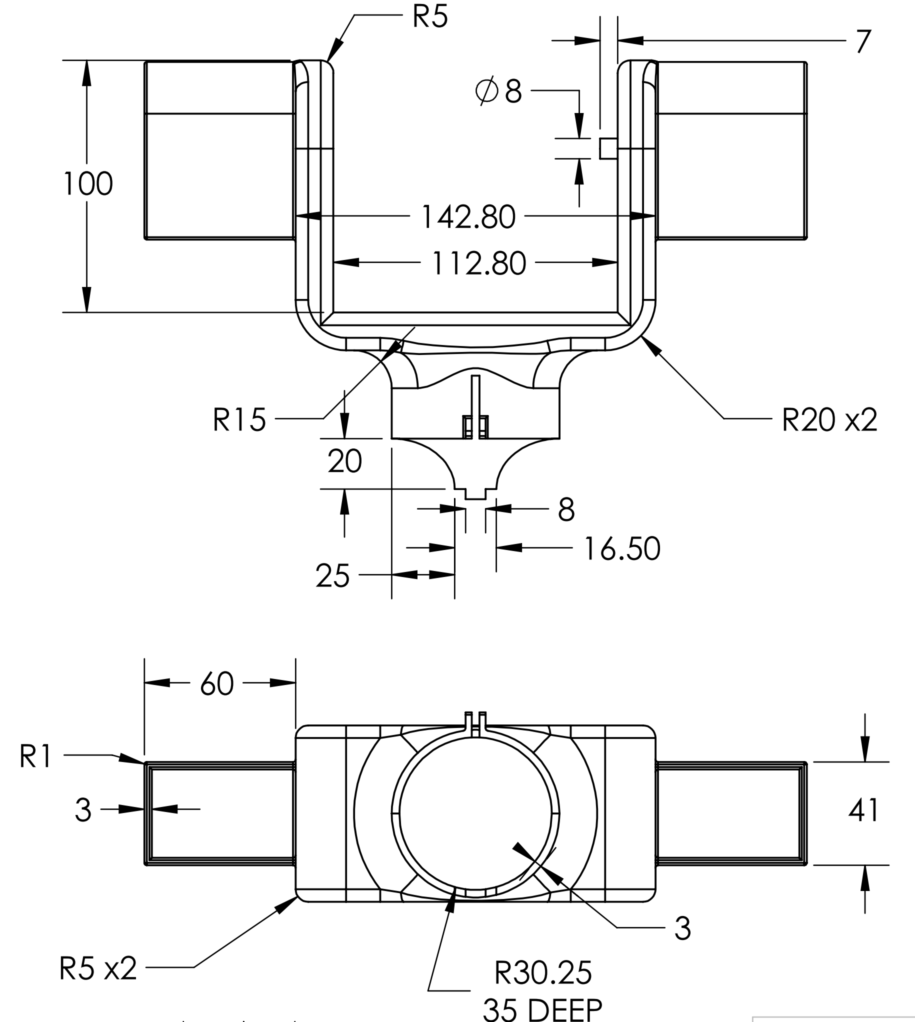


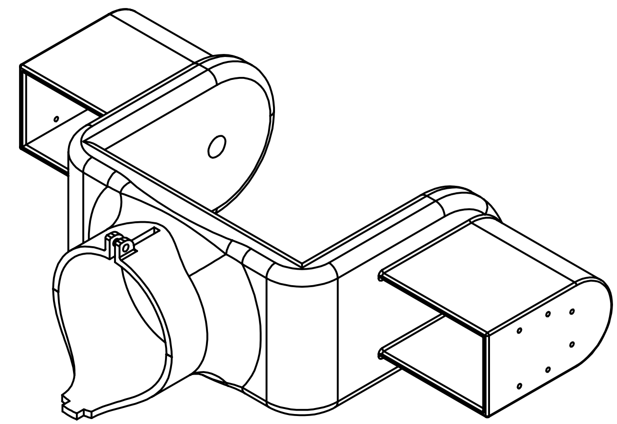

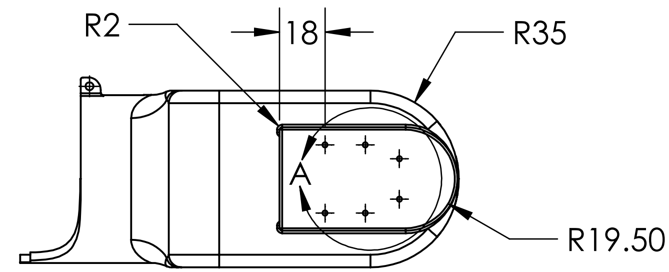


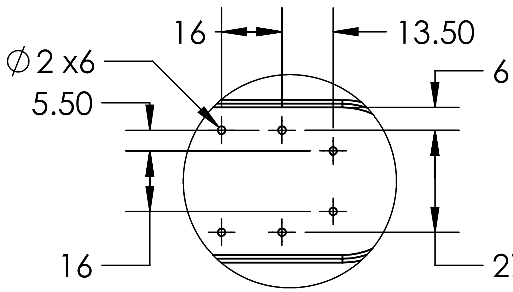


DETAIL A
SCALE 1 : 2

| | | | |
|---|---|---|---|
| UNLESS OTHERWISE SPECIFIED: | | NAME | DATE |
| DIMENSIONS ARE IN MILLIMETERS | DRAWN | Ryan W. | 11/13/2019 |
| TOLERANCES: ±3.0 | CHECKED | | |
| | ENG APPR. | | |
| | MFG APPR. | | |
| INTERPRET GEOMETRIC TOLERANCING PER: | Q.A. | | |
| MATERIAL PLA, 30% Infill | COMMENTS: | | |
| FINISH N/A | | | |
| DO NOT SCALE DRAWING | | | |

TITLE: Link 2_b

| SIZE | DWG. NO. | REV |
|---|---|---|
| A | | 1.0 |

| SCALE: 1:3 | WEIGHT: | SHEET 7 OF 13 |
|---|---|---|

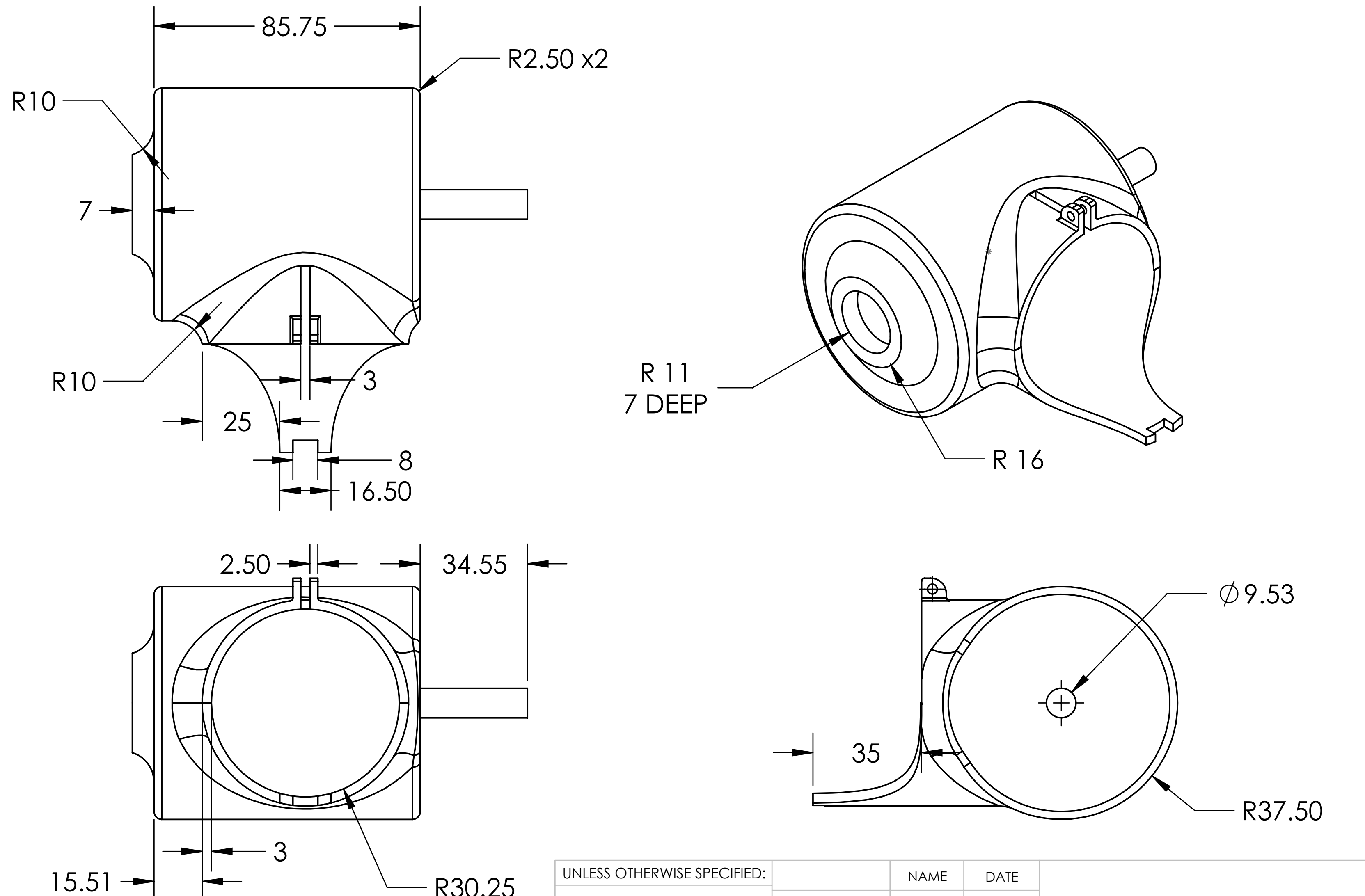


| UNLESS OTHERWISE SPECIFIED: | | NAME | DATE | |
|---|---|---|---|---|
| DIMENSIONS ARE IN MILLIMETERS | DRAWN | Ryan W. | 11/11/2019 | TITLE: |
| TOLERANCES: ±3.0 | CHECKED | | | Link 3_a |
| | ENG APPR. | | | |
| | MFG APPR. | | | |
| | Q.A. | | | |
| INTERPRET GEOMETRIC TOLERANCING PER: | COMMENTS: | | | |
| MATERIAL PLA, 30% Infill | | | | SIZE A — DWG. NO. — REV 1.0 |
| FINISH N/A | | | | |
| DO NOT SCALE DRAWING | | | | SCALE: 1:2 — WEIGHT: — SHEET 8 OF 13 |

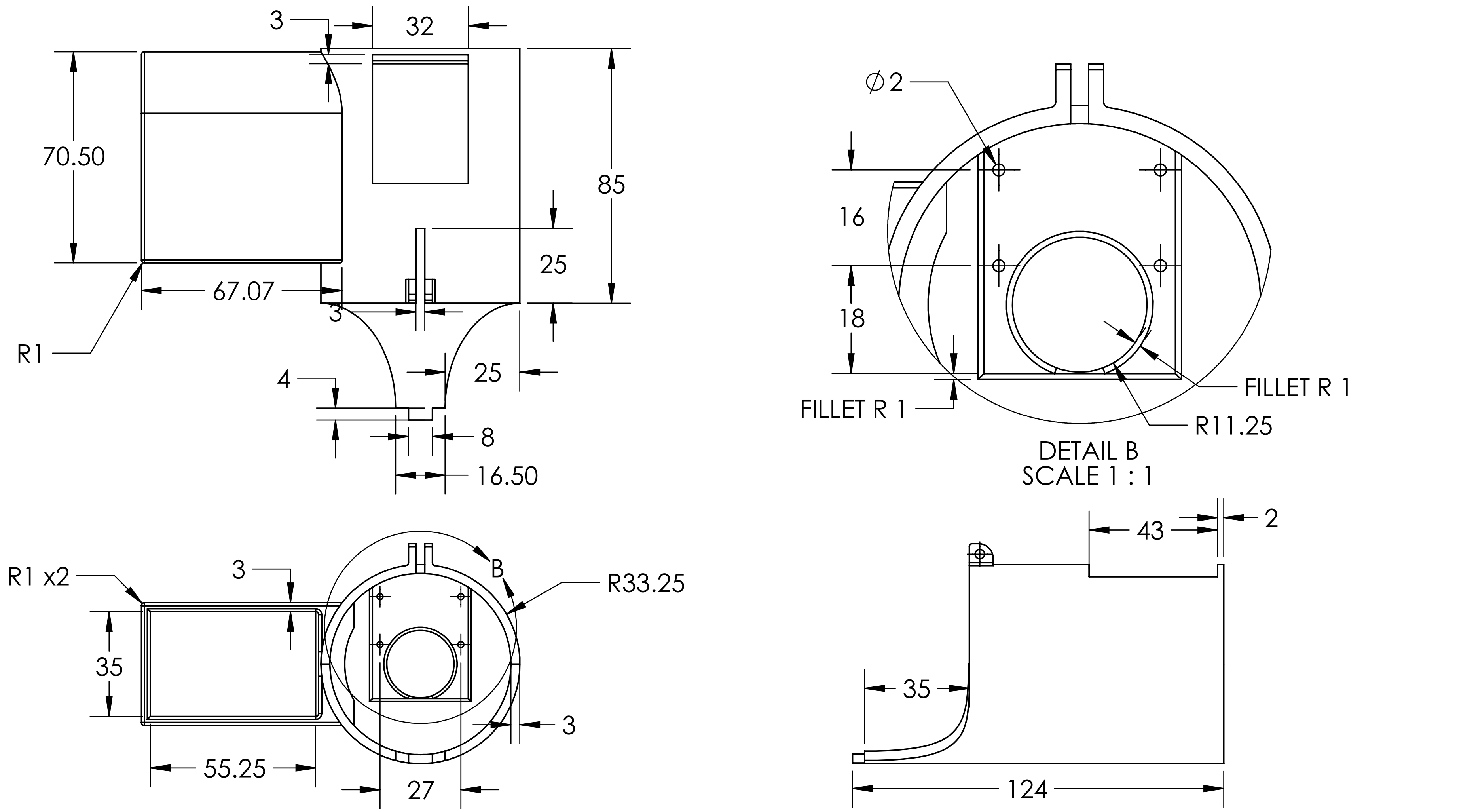


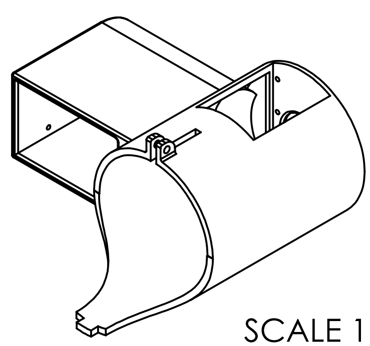

SCALE 1:3

| UNLESS OTHERWISE SPECIFIED: | | NAME | DATE | |
|---|---|---|---|---|
| DIMENSIONS ARE IN MILLIMETERS<br>TOLERANCES: ±3.0 | DRAWN | Ryan W. | 11/15/2019 | TITLE: Link 3_b |
| | CHECKED | | | |
| | ENG APPR. | | | |
| | MFG APPR. | | | |
| INTERPRET GEOMETRIC TOLERANCING PER: | Q.A. | | | |
| MATERIAL PLA, 30% Infill | COMMENTS: | | | SIZE A |
| FINISH N/A | | | | DWG. NO. |
| DO NOT SCALE DRAWING | | | | REV 1.0 |
| | | | | SCALE: 1:2 |
| | | | | WEIGHT: |
| | | | | SHEET 9 OF 13 |

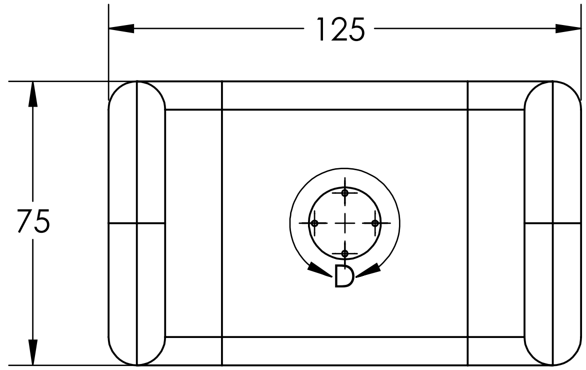


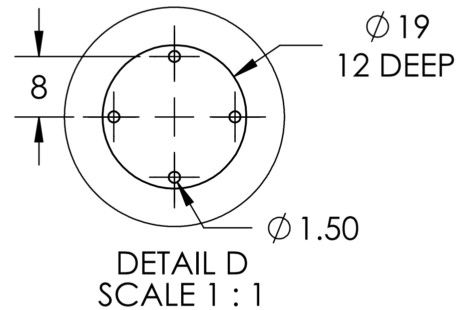


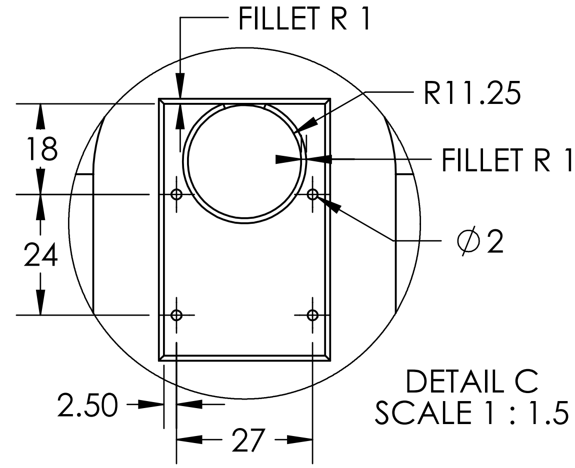


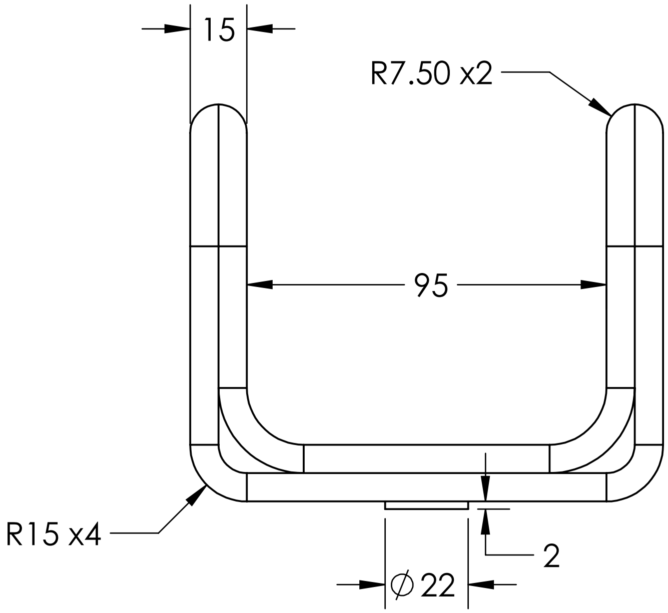


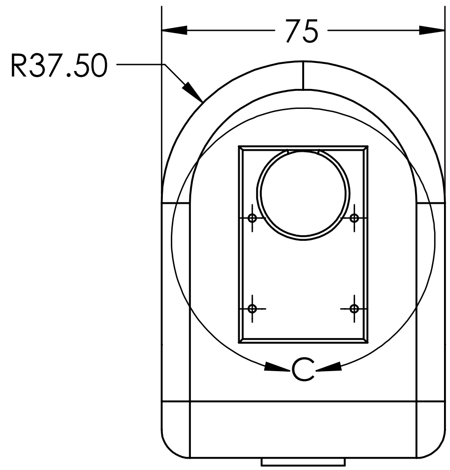


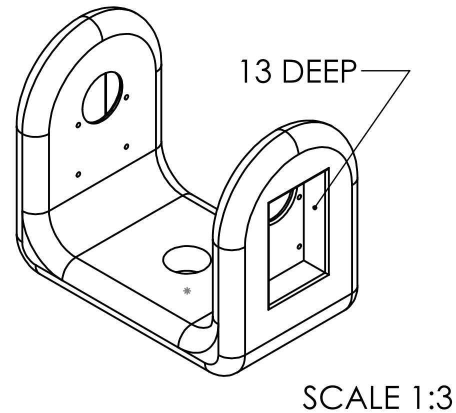


| | | | | |
|---|---|---|---|---|
| UNLESS OTHERWISE SPECIFIED: | | NAME | DATE | |
| DIMENSIONS ARE IN MILLIMETERS<br>TOLERANCES: ±3.0 | DRAWN | Ryan W. | 11/11/2019 | TITLE: Link 4 |
| | CHECKED | | | |
| | ENG APPR. | | | |
| | MFG APPR. | | | |
| | Q.A. | | | |
| INTERPRET GEOMETRIC TOLERANCING PER: | COMMENTS: | | | |
| MATERIAL PLA, 30% Infill | | | | SIZE A, DWG. NO., REV 1.0 |
| FINISH N/A | | | | |
| DO NOT SCALE DRAWING | | | | SCALE: 1:2, WEIGHT:, SHEET 10 OF 13 |

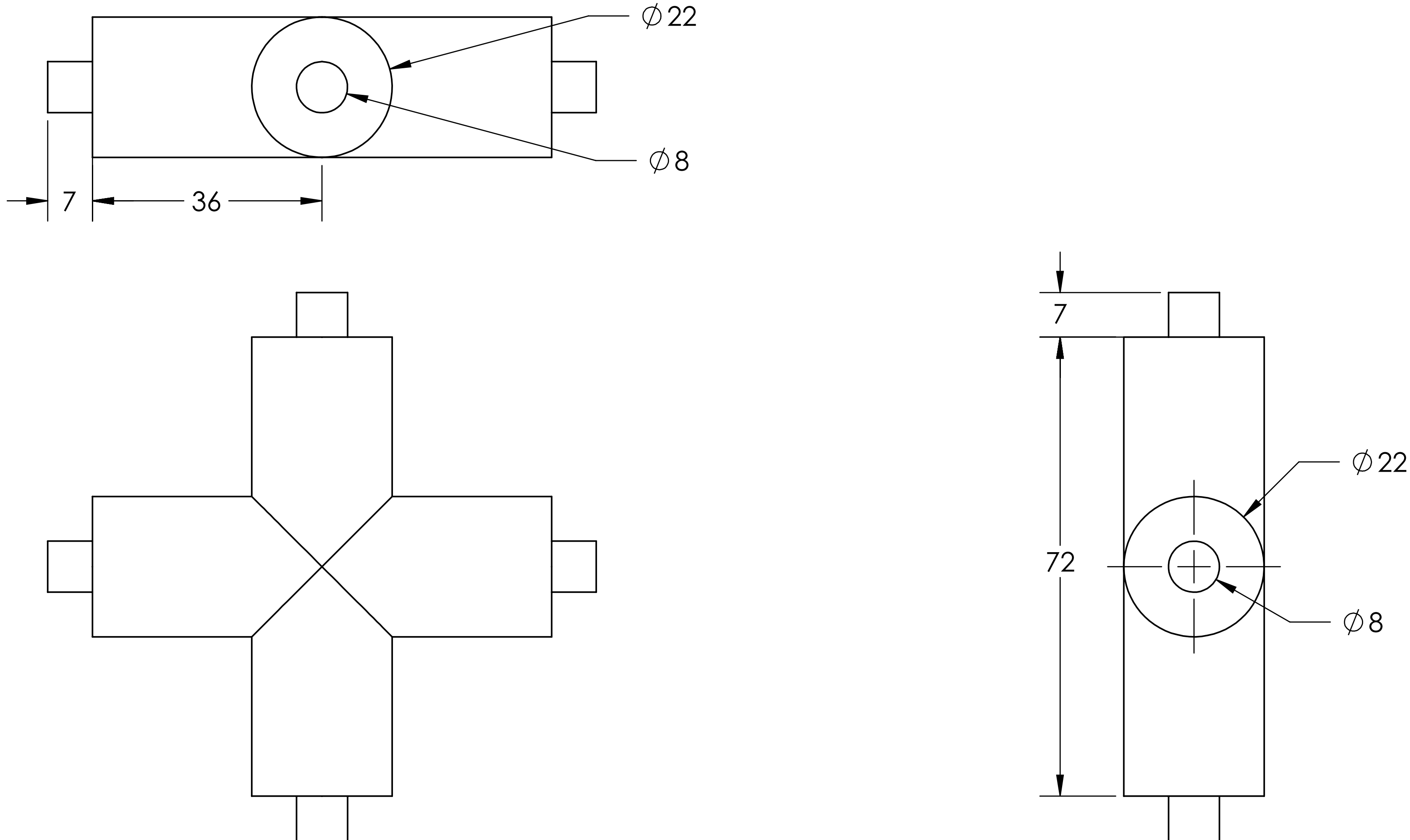


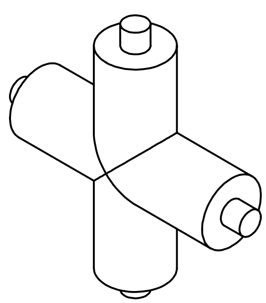

SCALE 1:2

| UNLESS OTHERWISE SPECIFIED: | | NAME | DATE | |
|---|---|---|---|---|
| DIMENSIONS ARE IN MILLIMETERS | DRAWN | Ryan W. | 11/8/2019 | TITLE: |
| TOLERANCES: ±3.0 | CHECKED | | | Wrist Differential Crossbar |
| | ENG APPR. | | | |
| | MFG APPR. | | | |
| INTERPRET GEOMETRIC TOLERANCING PER: | Q.A. | | | |
| MATERIAL PLA, 30% Infill | COMMENTS: | | | SIZE A |
| FINISH N/A | | | | DWG. NO. |
| DO NOT SCALE DRAWING | | | | REV 1.0 |
| | | | | SCALE: 1:1 |
| | | | | WEIGHT: |
| | | | | SHEET 11 OF 13 |

2 | 1

B | B

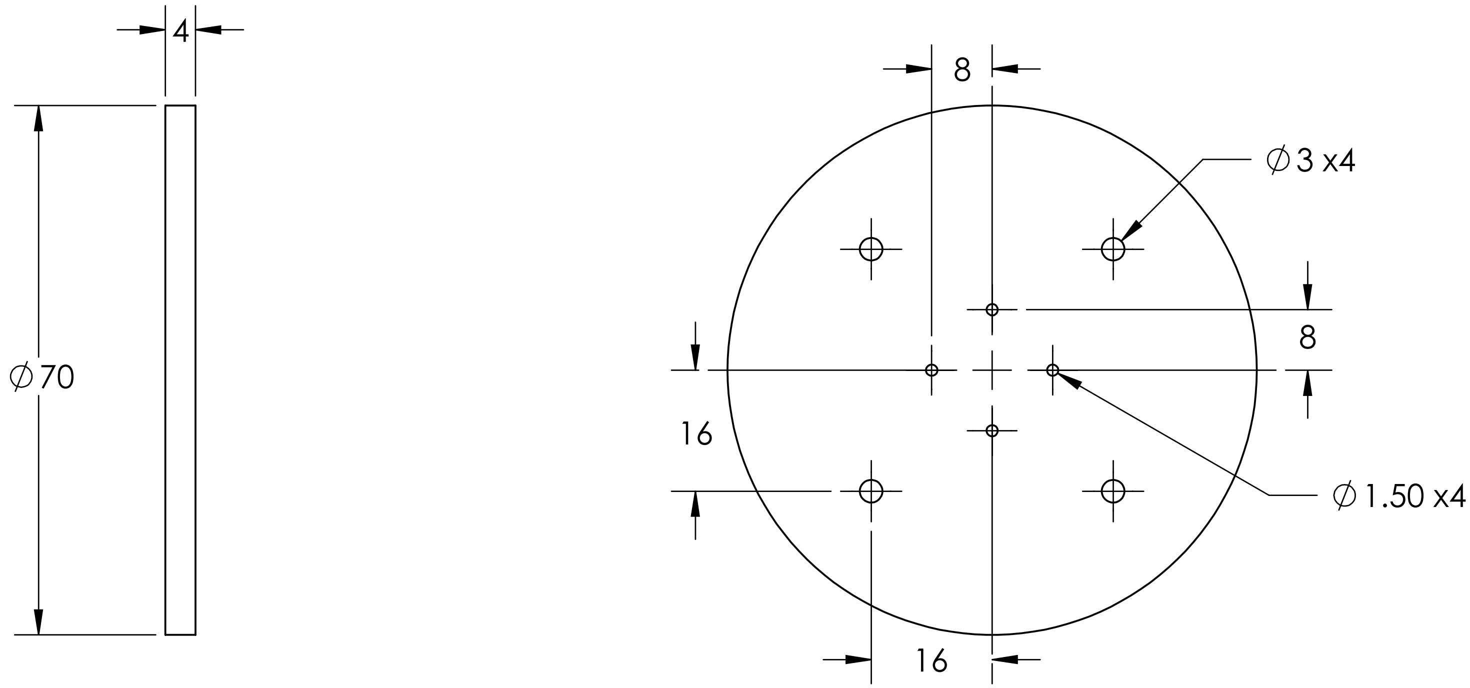


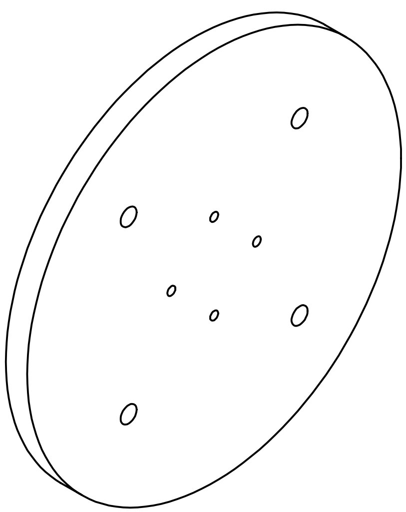

A | A

| UNLESS OTHERWISE SPECIFIED: | | NAME | DATE | |
|---|---|---|---|---|
| DIMENSIONS ARE IN MILLIMETERS<br>TOLERANCES: ±3.0 | DRAWN | Ryan W. | 11/8/2019 | TITLE:<br>Wrist Connection Plate |
| | CHECKED | | | |
| | ENG APPR. | | | |
| | MFG APPR. | | | |
| | Q.A. | | | |
| INTERPRET GEOMETRIC TOLERANCING PER: | COMMENTS: | | | |
| MATERIAL<br>PLA, 20% Infill | Connection plate between smart servo and bevel gear in the wrist. | | | SIZE A \| DWG. NO. \| REV 1.0 |
| FINISH<br>N/A | | | | |
| DO NOT SCALE DRAWING | | | | SCALE: 1:2 \| WEIGHT: \| SHEET 12 OF 13 |

2 | 1

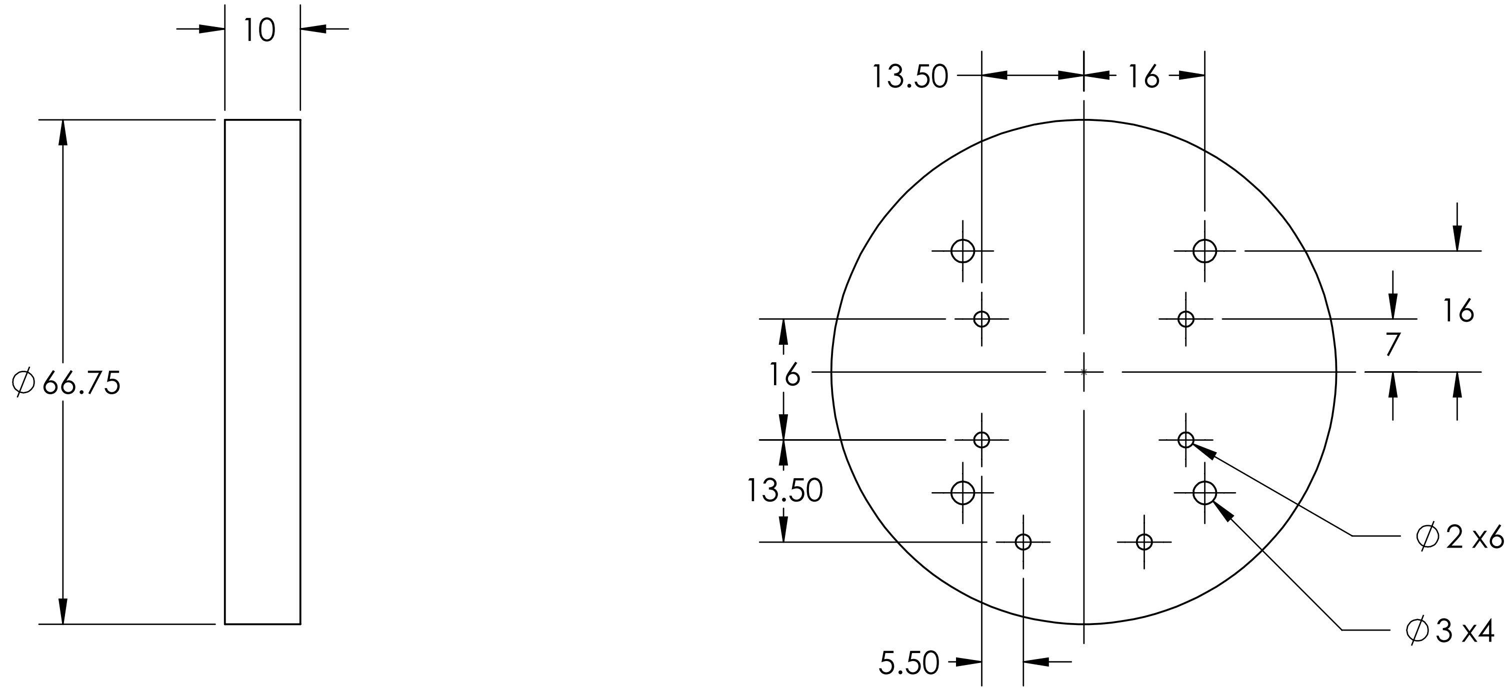


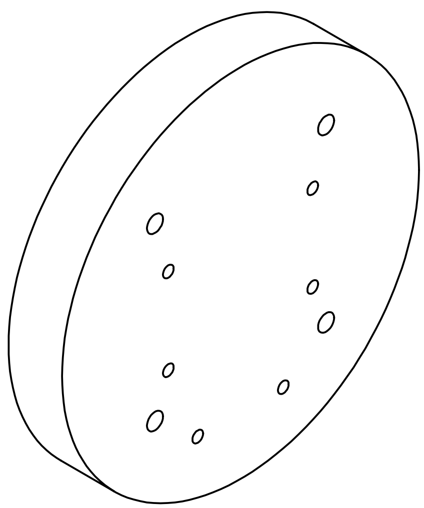

| UNLESS OTHERWISE SPECIFIED: | | NAME | DATE | |
|---|---|---|---|---|
| DIMENSIONS ARE IN MILLIMETERS | DRAWN | Ryan W. | 11/11/2019 | TITLE: |
| TOLERANCES: ±3.0 | CHECKED | | | End Effector |
| | ENG APPR. | | | |
| | MFG APPR. | | | |
| INTERPRET GEOMETRIC TOLERANCING PER: | Q.A. | | | |
| MATERIAL PLA, 20% Infill | COMMENTS: | | | SIZE A · DWG. NO. · REV 1.0 |
| FINISH N/A | | | | |
| DO NOT SCALE DRAWING | | | | SCALE: 1:2 · WEIGHT: · SHEET 13 OF 13 |

## iii Salient Code

Listing 1: Actuator Dynamics MATLAB Code

```matlab
% dynamixel motor model experiment
close all;clear;clc

% test loads mass moments of inertia
m = [.146 .088 0.108];          % mass (kg)
b = [.61277 .37227 0.28257];    % length (m)
h = [.01915 0.01915 0.0299];    % height (m)
J = (1/12)*m.*(h.^2 + b.^2);

% path to csv files relative to script
datapath = 'data/AX12A/';
files = dir(strcat(datapath,'*.csv'));
numFiles = length(files);
% initialize variables
[damp, wn, Tp] = deal(zeros(numFiles,1));

for ii = 1:numFiles
    % load experimental data, skip 5 header lines
        M = csvread(strcat(datapath, files(ii).name),5,0);
    % clean data by removing outliers
        nani = (find(diff(M(:,1)) > 100));
        M(nani,:) = [];
    % show response
         figure();
         plot(M(:,1),M(:,2))
         title('Experimental Data')
    % find % OS
        peak = max(M(:,2));                        % peak value
        peaki = find(M(:,2)==peak, 1, 'first');    % peak value index
        ss = M(end,2);                             % steady state
        os = ((peak - ss) / ss) * 100;             % % OS
    % damping ratio
        damp(ii) = -log(os/100) / sqrt(pi^2 + log(os/100)^2);
    % find where the motor begins responding
        start = M(find(diff(M(:,2)) > 1, 1, 'first'), 1);
    % time to peak
        Tp(ii) = (M(peaki,1) - start) / 1000;
    % natural frequency
        wn(ii) = pi / (sqrt(1 - damp(ii)^2)*Tp(ii));
end

sol = zeros(4,1);
```

```
% no load case, 2*zeta*omega_n
sol(1) = 2*mean(damp(end-2:end))*mean(wn(end-2:end));
% no load case, omega_n^2
sol(2) = mean(wn(end-2:end))^2;

% obtain average damping ratio and natural frequencies for load cases
zeta = [mean(damp(1:3));mean(damp(4:6));mean(damp(7:9))];
omegan = [mean(wn(1:3));mean(wn(4:6));mean(wn(7:9))];

alpha = 2.*zeta.*omegan;
beta = omegan.^2;
A = zeros(3,2);
b = zeros(3,1);

for jj = 1:3
    A(jj,:) = [1, -(alpha(jj)*J(jj) + beta(jj)*J(jj))];
    b(jj) = alpha(jj) + beta(jj);
end

sol(3:4) = A \ b;
```

Listing 2: Forward Kinematics MATLAB Function

```
function [r6,T6]= MeiosisFK(theta)

    %       Mapping between joint space and motor space
    N = 10;         %Gear Ratio
    A = [ 1/(2*N), 1/(2*N),   0, 0,   0,   0;
          1/(2*N),-1/(2*N),   0, 0,   0,   0;
                0,       0,-1/N, 0,   0,   0;
                0,       0,   0, 1,   0,   0;
                0,       0,   0, 0,-1/2, 1/2;
                0,       0,   0, 0, 1/2, 1/2];
    gamma = A*theta;

%     %Define Constants
%     LB = 12.275;
%     L1 = 0;
%     L2 = 25;
%     L3 = 20;
%     L4 = 7.2;
%     L5 = 0;
```

```
%     L6 = 5.3;

    %Relative Positions
    rBfromI = [ 0.00000000; 0.00000000; 0.00000000];
    r1fromB = [ 0.00000000; 0.00000000; 0.12275000];
    r2from1 = [ 0.00000000; 0.00000000; 0.00000000];
    r3from2 = [ 0.00000000; 0.25000000; 0.00000000];
    r4from3 = [ 0.00000000; 0.20000000; 0.00000000];
    r5from4 = [ 0.00000000; 0.07000000; 0.00000000];
    r6from5 = [ 0.00000000; 0.04750000; 0.00000000];
    %r7from6 = [0;       0;       0]; % dist. from 3rd wrist coor. frame to the end effector is 5.25 cm

    %Orientations wrt I:
    T1 = rotz(gamma(1));
    T2 = T1*rotx(gamma(2));
    T3 = T2*rotx(gamma(3));
    T4 = T3*roty(gamma(4));
    T5 = T4*rotx(gamma(5));
    T6 = T5*roty(gamma(6));

    %Positions wrt I:
    %rB = rBfromI;
    r1 = r1fromB;
    r2 = r1 + T1*r2from1;
    r3 = r2 + T2*r3from2;
    r4 = r3 + T3*r4from3;
    r5 = r4 + T4*r5from4;
    r6 = r5 + T5*r6from5;

end
```

Listing 3: Inverse Kinematics MATLAB Function

```
function [theta, error] = MeiosisIK(pos,R)

    eOff = [0;47.5;0];
    npos = pos - R*eOff;
    xc = npos(1);
    yc = npos(2);
    zc = npos(3);
    L1 = 122.75;
```

```matlab
    d = 0;
    L2 = 250;
    L3 = 270;

    % Inverse Position
    if (xc^2 + yc^2 -d^2) < 0
        theta = 1000*[1;1;1;1;1;1];
        error = 1;
    else
        t1 = atan2(yc,xc) - atan2(d,sqrt(xc^2 + yc^2 -d^2)) - pi/2;
        D = (xc^2 + yc^2 - d^2 + (zc - L1)^2 - L2^2 - L3^2)/(2*L2*L3);
        t3 = atan2(-sqrt(1-D^2),D);
        t2 = atan2(zc - L1,sqrt(xc^2 + yc^2 - d^2)) - atan2(L3*sin(t3),L2 + L3*cos(t3));

        % Inverse Orientation
        T3 = rotz(t1)*rotx(t2)*rotx(t3);
        T = T3.'*R;
        t6 = atan2(T(2,1),-T(2,3));
        t4 = atan2(T(1,2),T(3,2));
        %t4 = atan2(sin(t4),cos(t4));

        if sin(t4) > -10e-6 && sin(t4) < 10e-6
            t5 = atan2(T(3,2)/cos(t4),T(2,2));
        else
            t5 = atan2(T(1,2)/sin(t4),T(2,2));
        end

        gamma = [t1,t2,t3,t4,t5,t6].';

        %       Mapping between joint space and motor space
        N = 10;         %Gear Ratio
%         B = [ N, N, 0, 0, 0, 0;
%               N,-N, 0, 0, 0, 0;
%               0, 0,-N, 0, 0, 0;
%               0, 0, 0, 1, 0, 0;
%               0, 0, 0, 0,-1, 1;
%               0, 0, 0, 0, 1, 1];
        A = [ 1/(2*N), 1/(2*N),   0, 0,    0,   0;
          1/(2*N),-1/(2*N),   0, 0,    0,   0;
                0,       0,-1/N, 0,    0,   0;
                0,       0,   0, 1,    0,   0;
                0,       0,   0, 0,-1/2, 1/2;
                0,       0,   0, 0, 1/2, 1/2];

```

```
        theta = A\gamma;
        error = 0;
    end
end
```